

Supporting Information

for

Salicylaldehyde derived piperazine functionalized hydrazone ligand-based Pt(II) complexes: Inhibition of EZH2-dependent tumorigenesis in pancreatic ductal adenocarcinoma, synergism with PARP inhibitors and enhanced apoptosis

Zhimin Lv^{a,#}, Amjad Ali^{b,c,#}, Cheng Zou^a, Zerui Wang^a, Minglu Ma^a, Na Cheng^a, Man Shad^{a,d}, Huifang Hao,^{a,d} Yongmin Zhang^{a,e,*} and Faiz-Ur Rahman^{a,*}

^aInner Mongolia University Research Center for Glycochemistry of Characteristic Medicinal Resources, Department of Chemistry and Chemical Engineering, Inner Mongolia University, Hohhot People's Republic of China

^bInstitute of Integrative Biosciences, CECOS University of IT and Emerging Sciences, Peshawar, KPK, Pakistan.

^cInstitute of Biomedical Sciences, School of Life Sciences, East China Normal University, 500 Dongchuan Road, Shanghai, 200241, People's Republic of China.

^dSchool of Life Sciences, Inner Mongolia University, Hohhot 010021, People's Republic of China

^eSorbonne Université, CNRS, Institut Parisien de Chimie Moléculaire, UMR 8232, 4 Place Jussieu, 75005 Paris, France.

[#]These authors contributed equally to this work.

*Corresponding Authors E-mail: Yongmin.zhang@upmc.fr (Y. Zhang), faiz@imu.edu.cn (F.-U. Rahman)

^1H and ^{13}C NMR spectra of all ligands

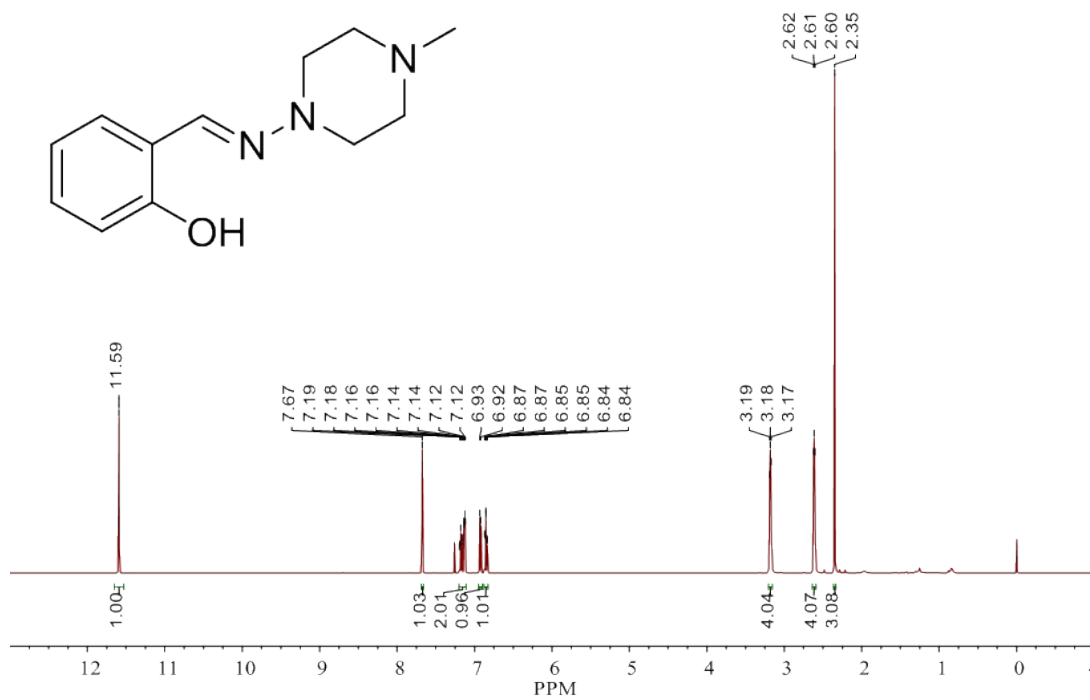


Fig. S1 ^1H NMR of L1 in CDCl_3 at 25°C

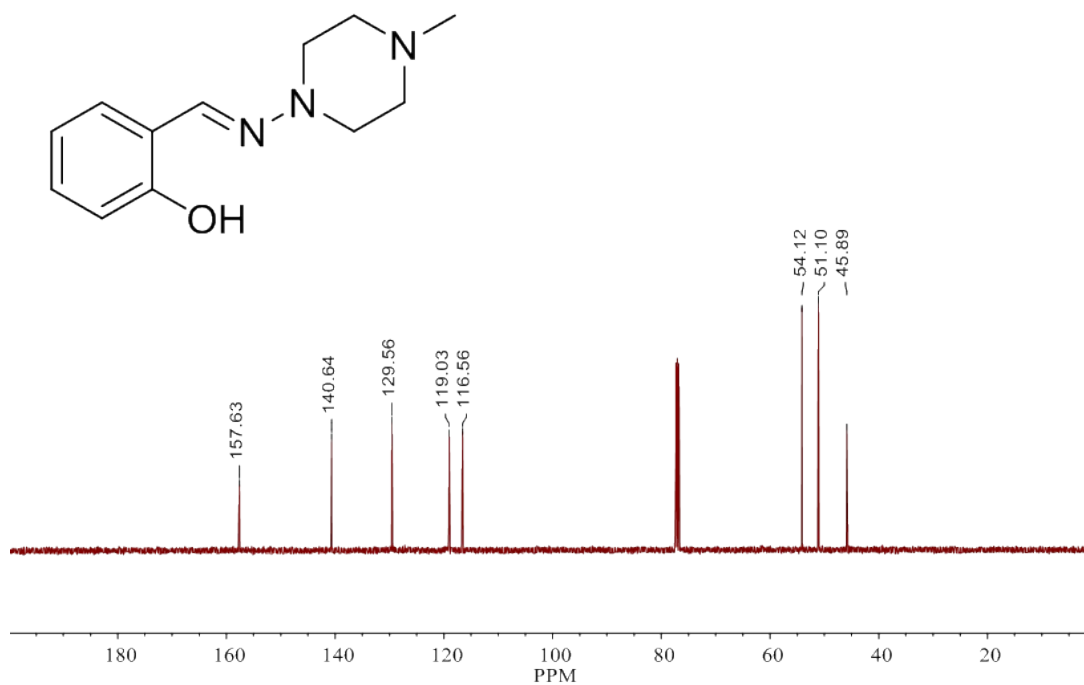


Fig. S2 ^{13}C NMR of L2 in CDCl_3 at 25°C

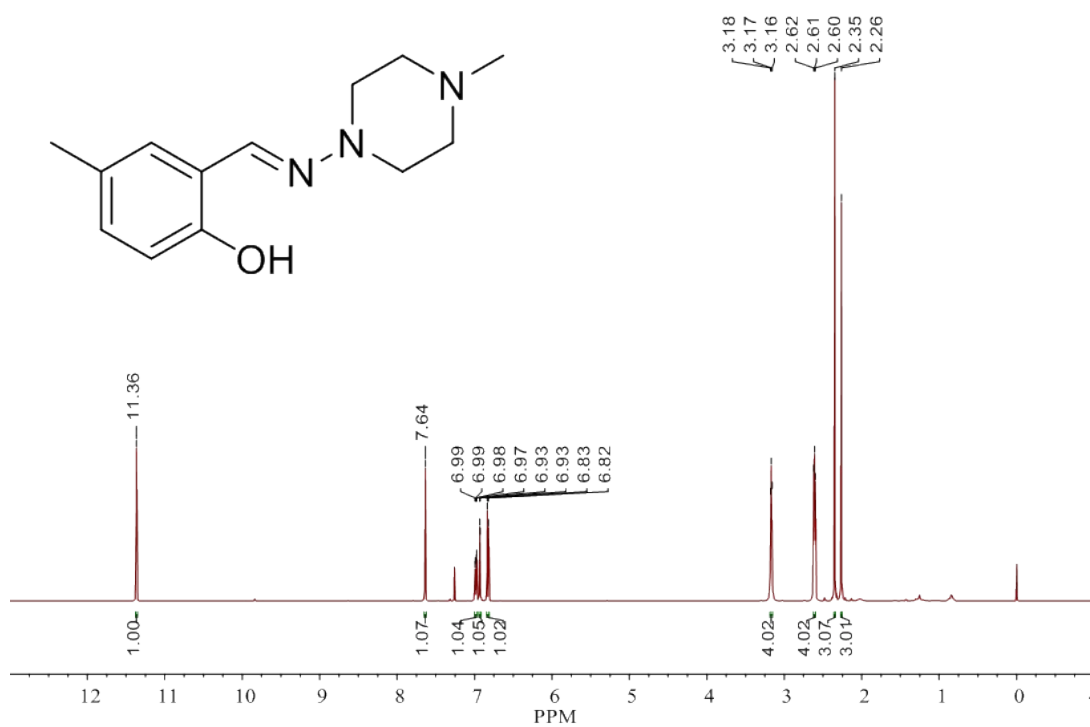


Fig. S3 ¹H NMR of L2 in CDCl₃ at 25°C

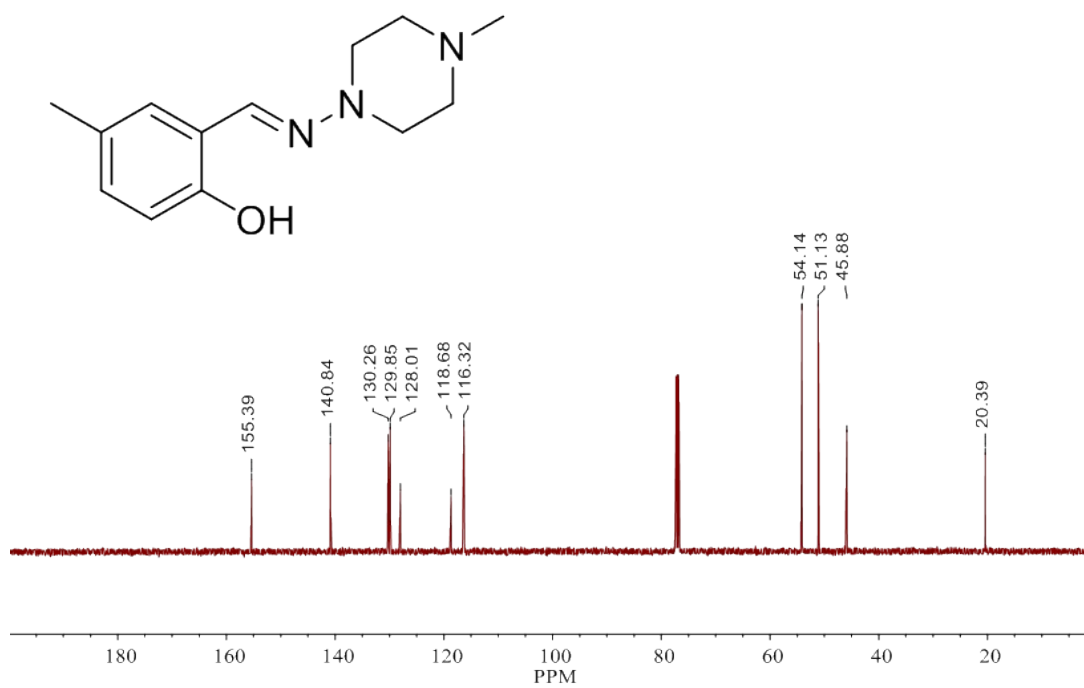


Fig. S4 ¹³C NMR of L2 in CDCl₃ at 25°C

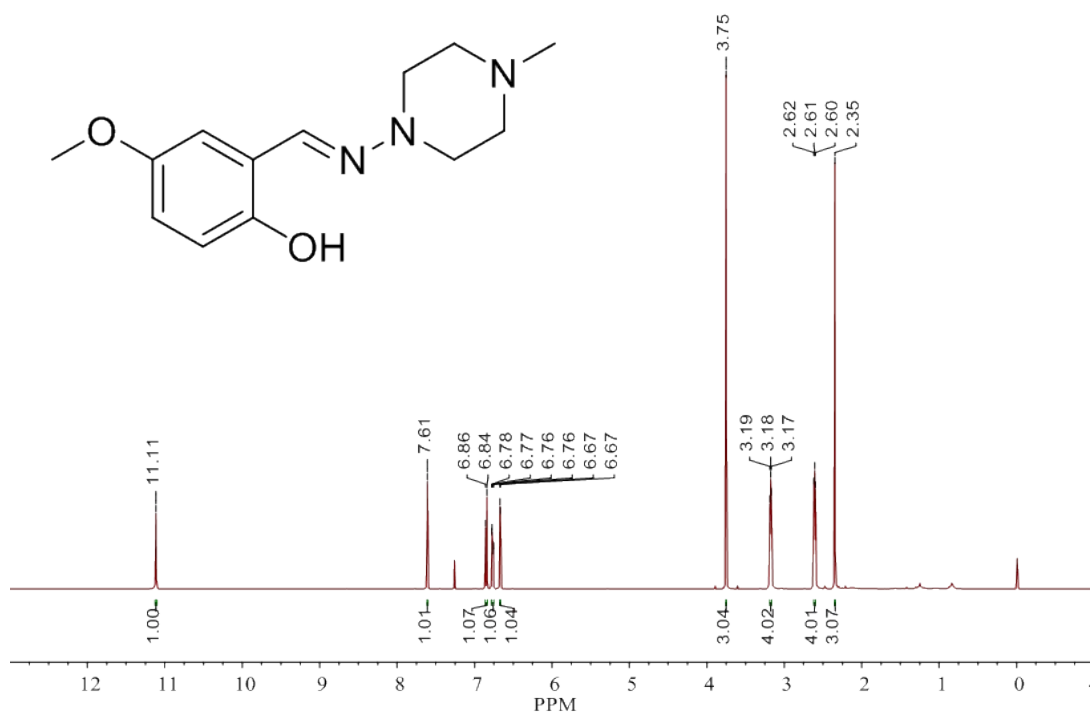


Fig. S5 ¹H NMR of L3 in CDCl₃ at 25°C

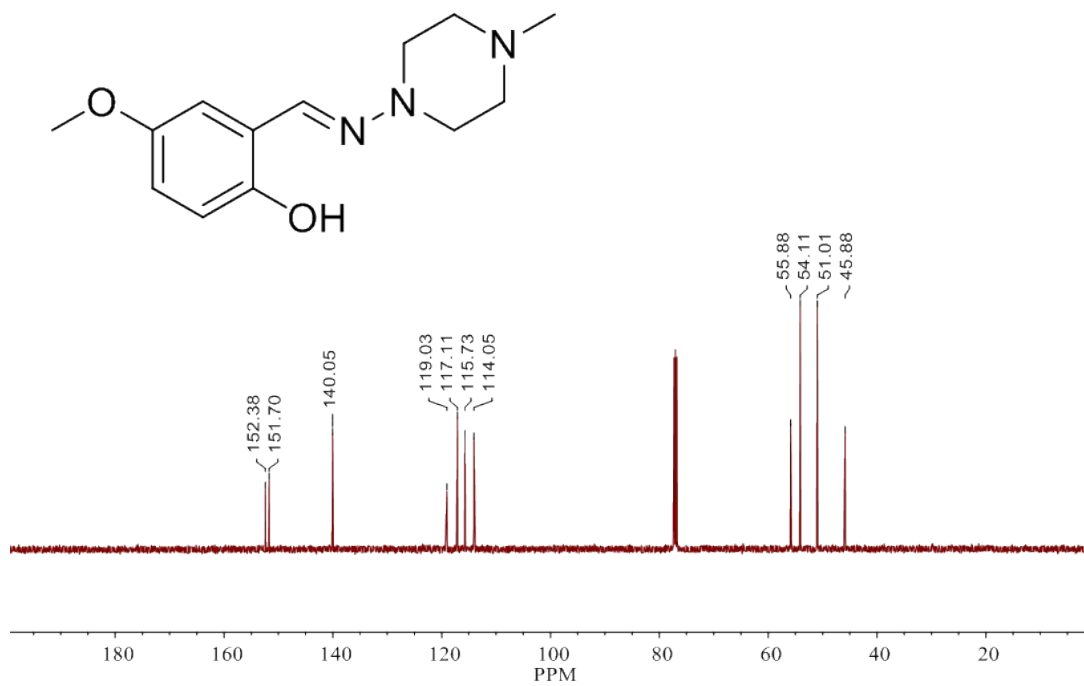


Fig. S6 ¹³C NMR of L3 in CDCl₃ at 25°C

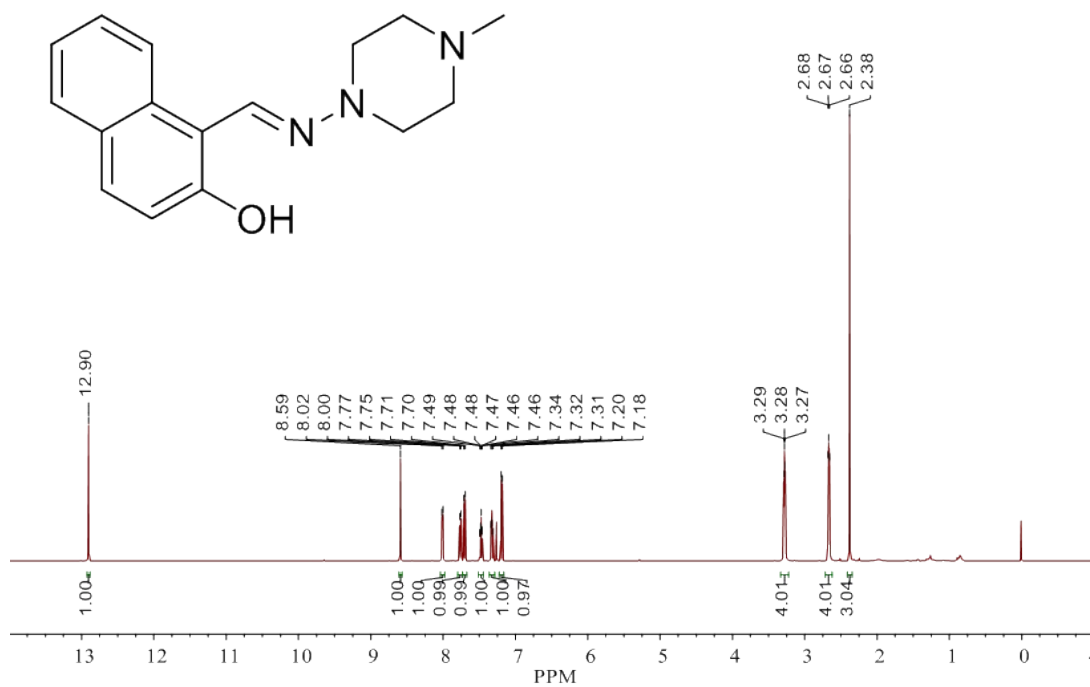


Fig. S7 ¹H NMR of L4 in CDCl₃ at 25°C

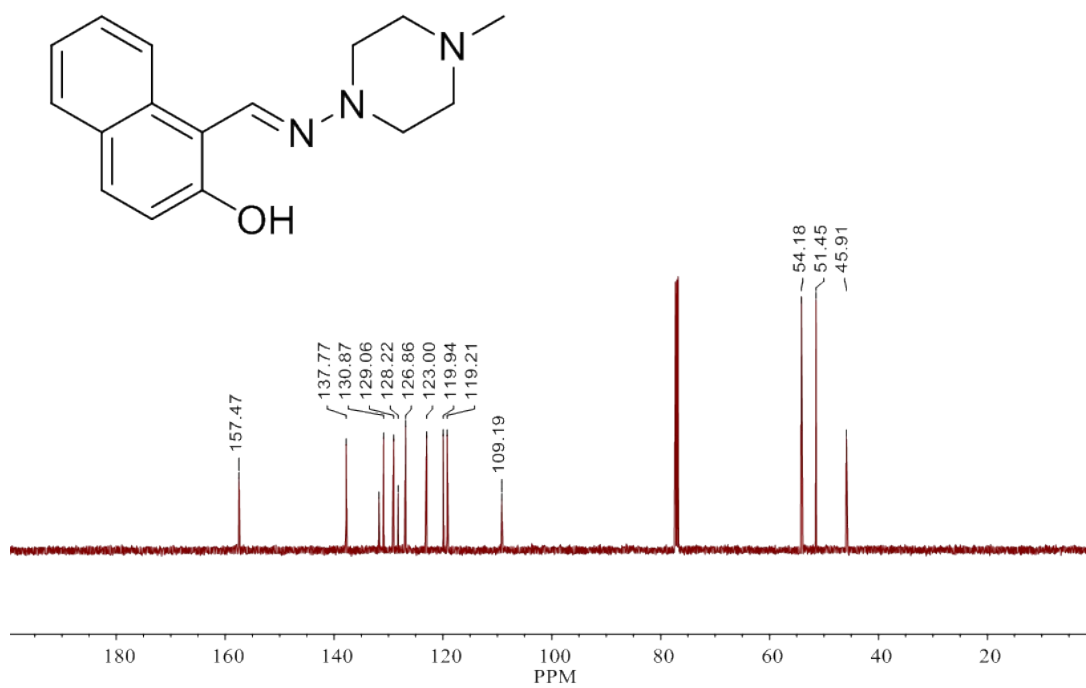


Fig. S8 ¹³C NMR of L4 in CDCl₃ at 25°C

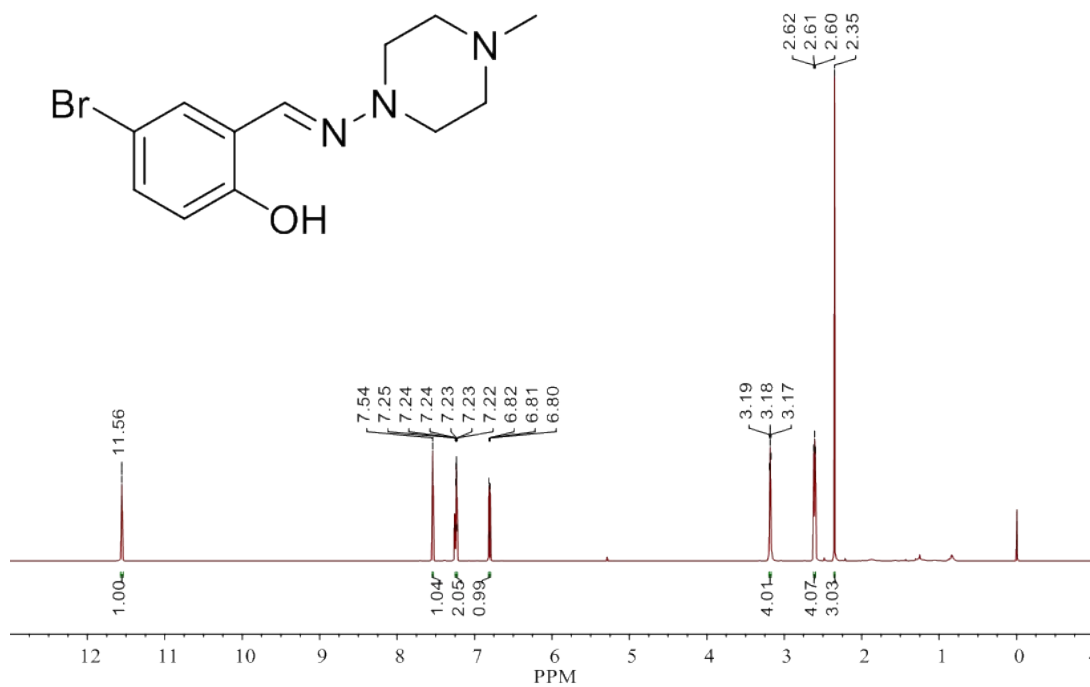


Fig. S9 ¹H NMR of L5 in CDCl₃ at 25°C

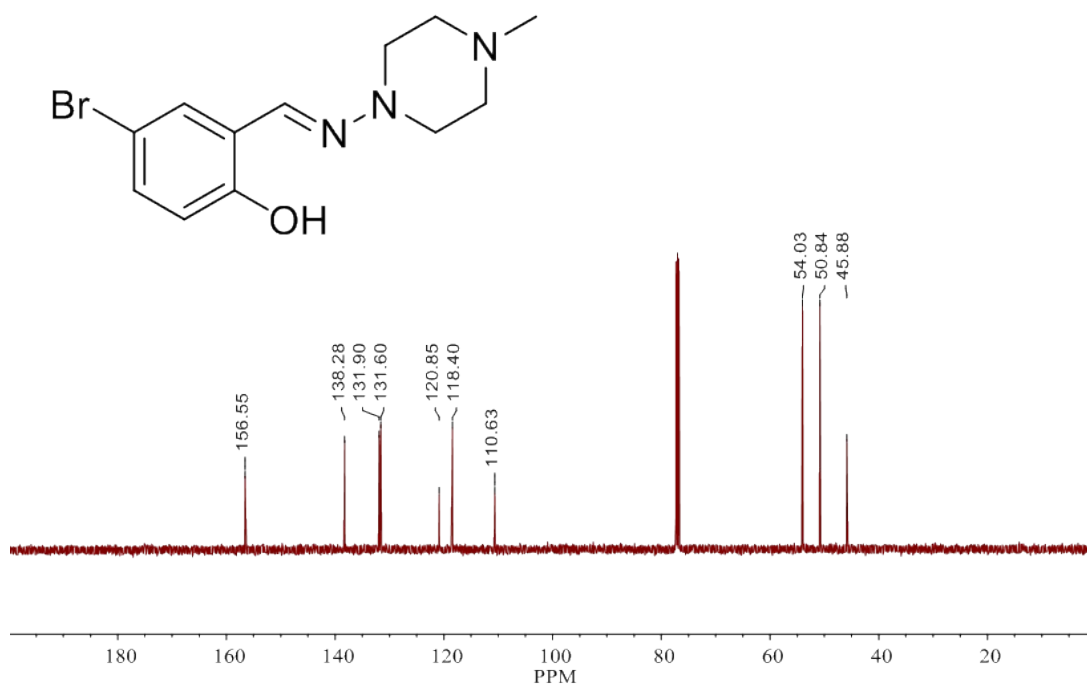


Fig. S10 ¹³C NMR of L5 in CDCl₃ at 25°C

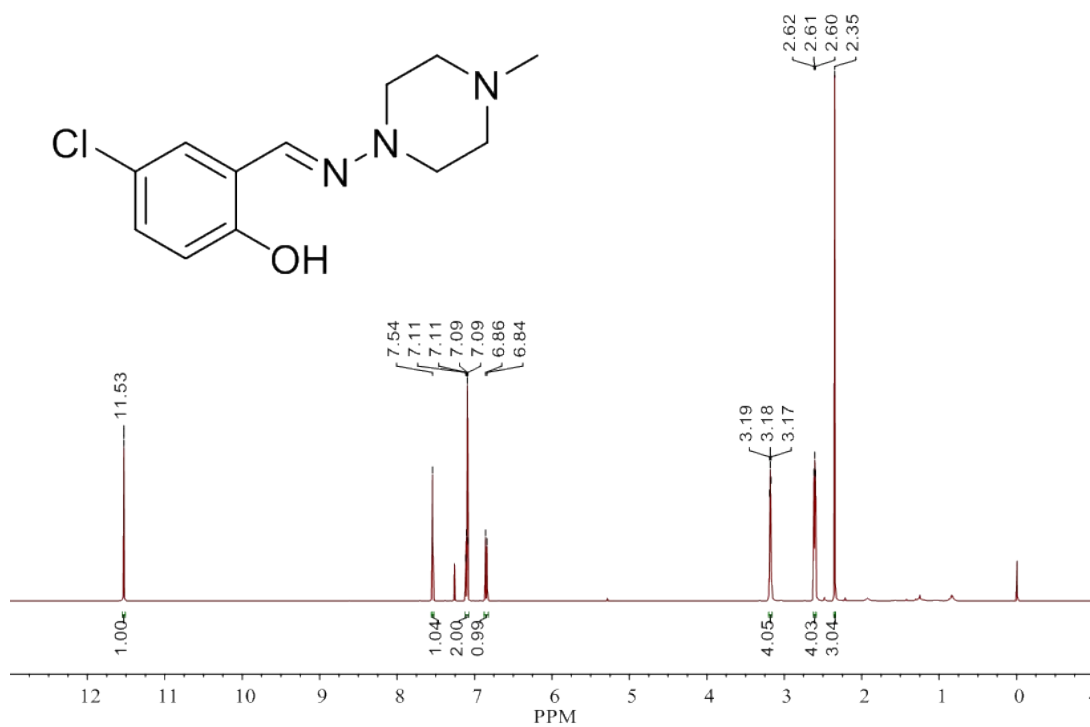


Fig. S11 ¹H NMR of L6 in CDCl₃ at 25°C

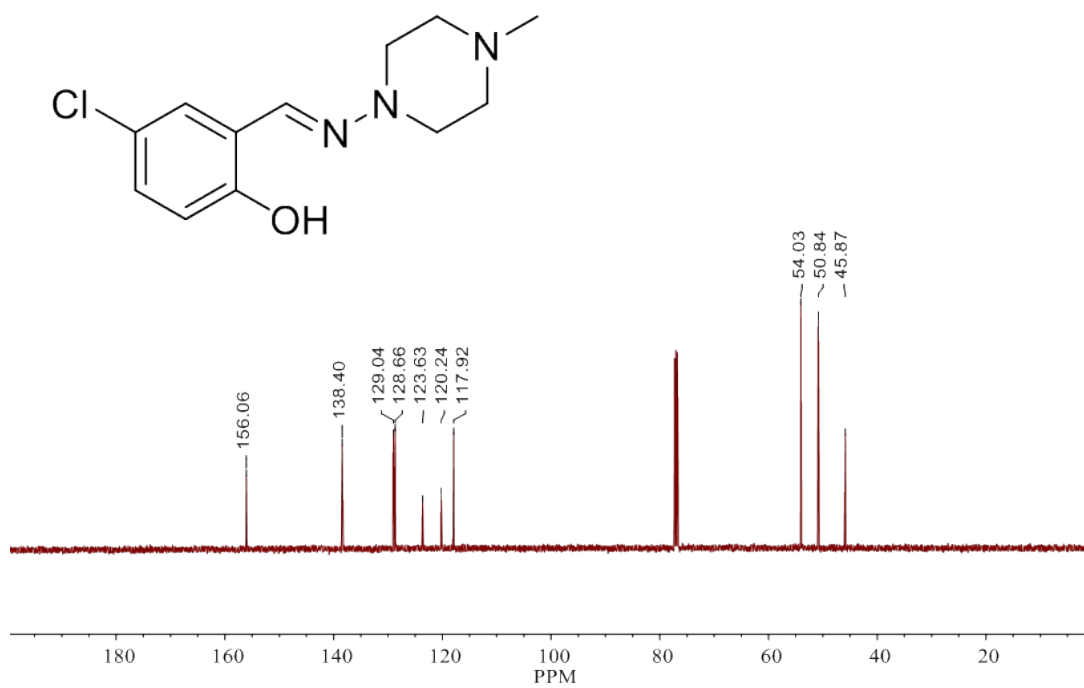


Fig. S12 ¹³C NMR of L6 in CDCl₃ at 25°C

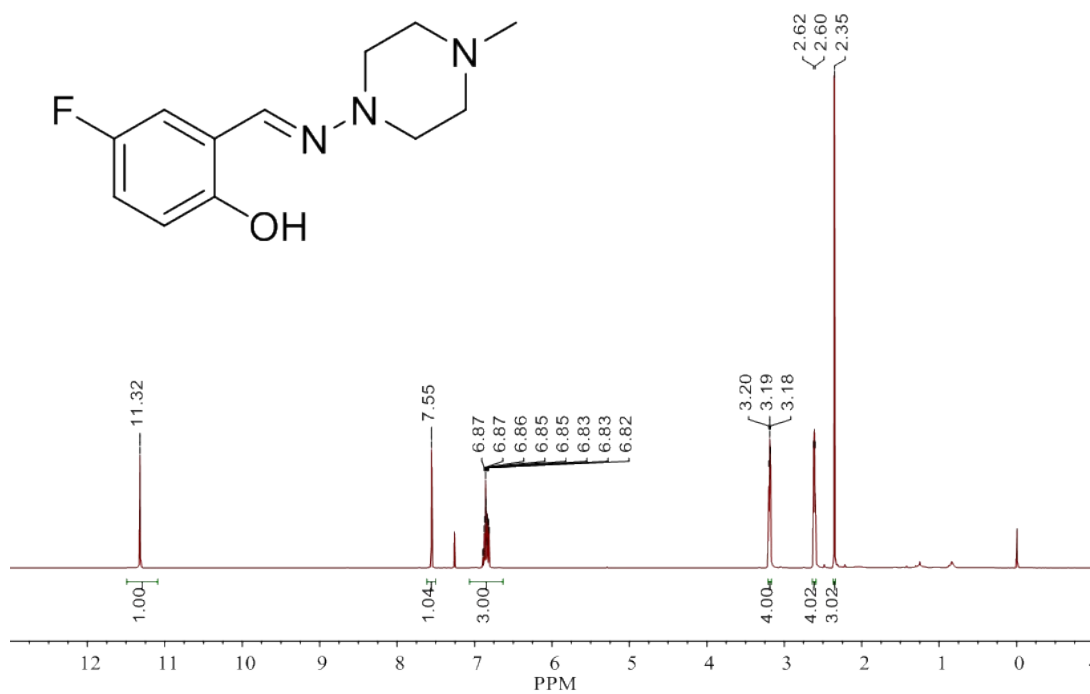


Fig. S13 ¹H NMR of L7 in CDCl₃ at 25°C

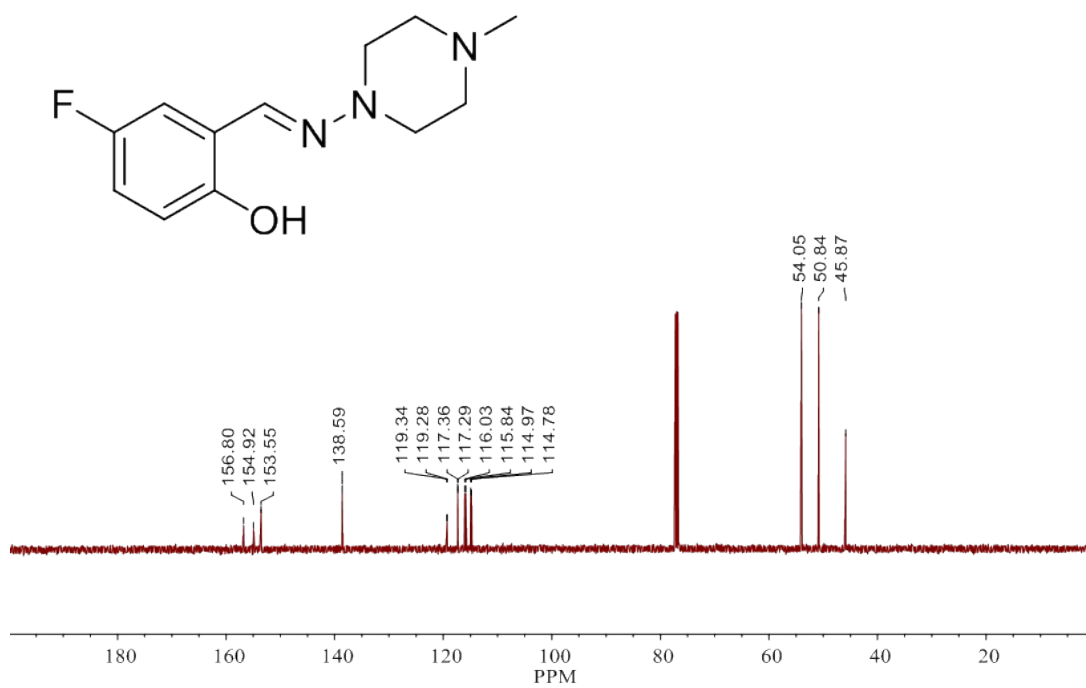


Fig. S14 ¹³C NMR of L7 in CDCl₃ at 25°C

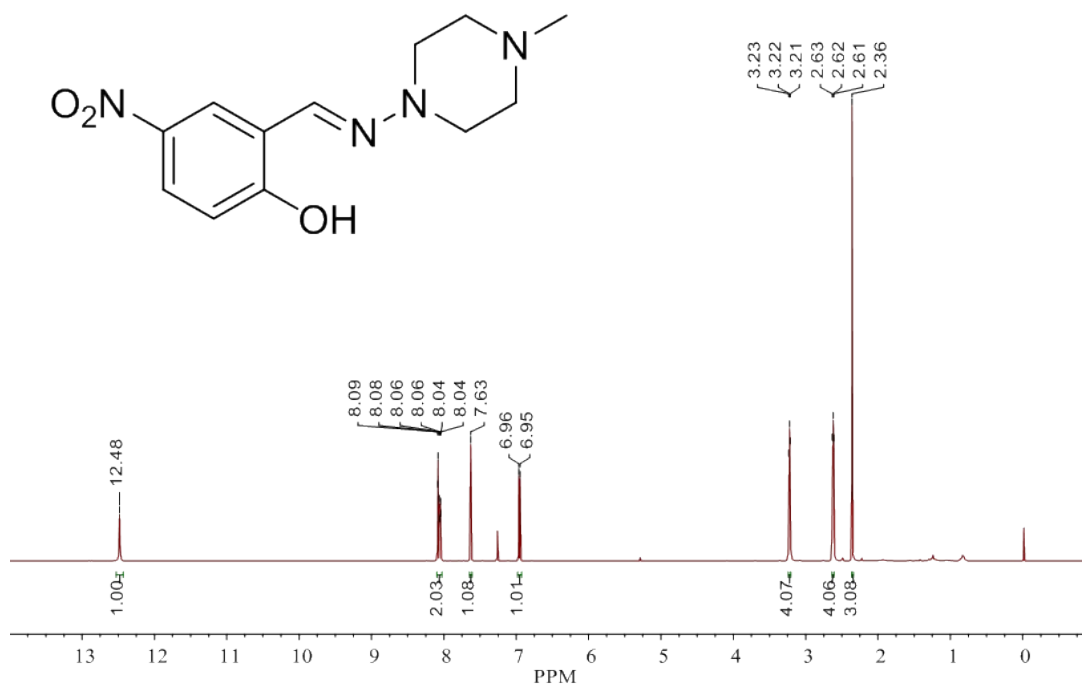


Fig. S15 ¹H NMR of L8 in CDCl₃ at 25°C

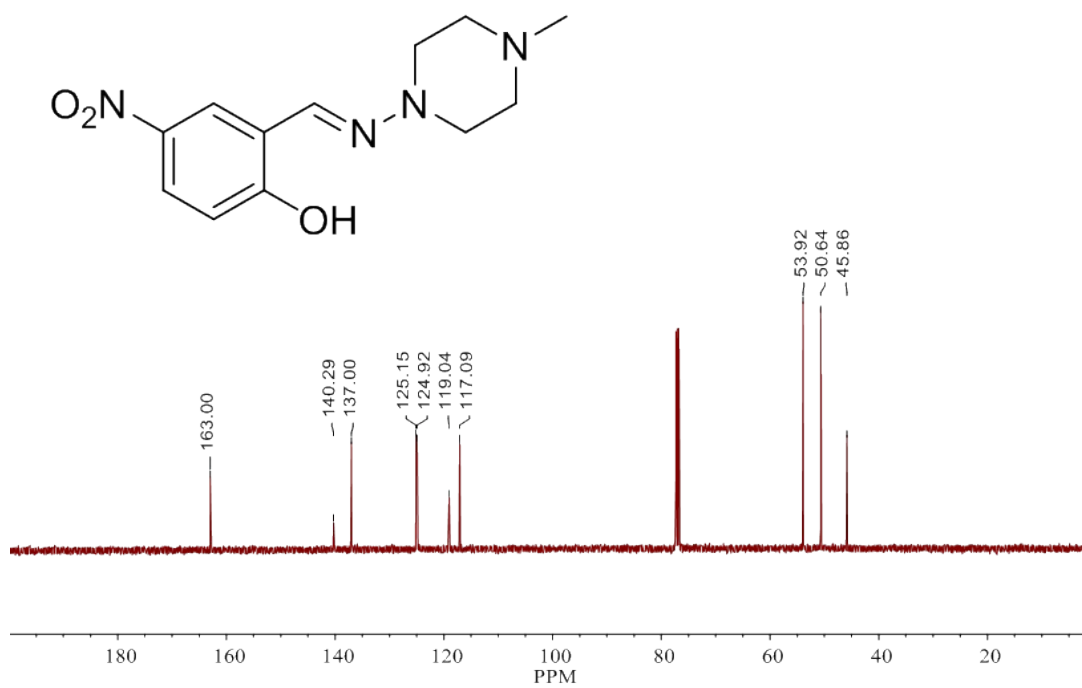


Fig. S16 ¹³C NMR of L8 in CDCl₃ at 25°C

^1H and ^{13}C NMR spectra of platinum complexes (C1-C8)

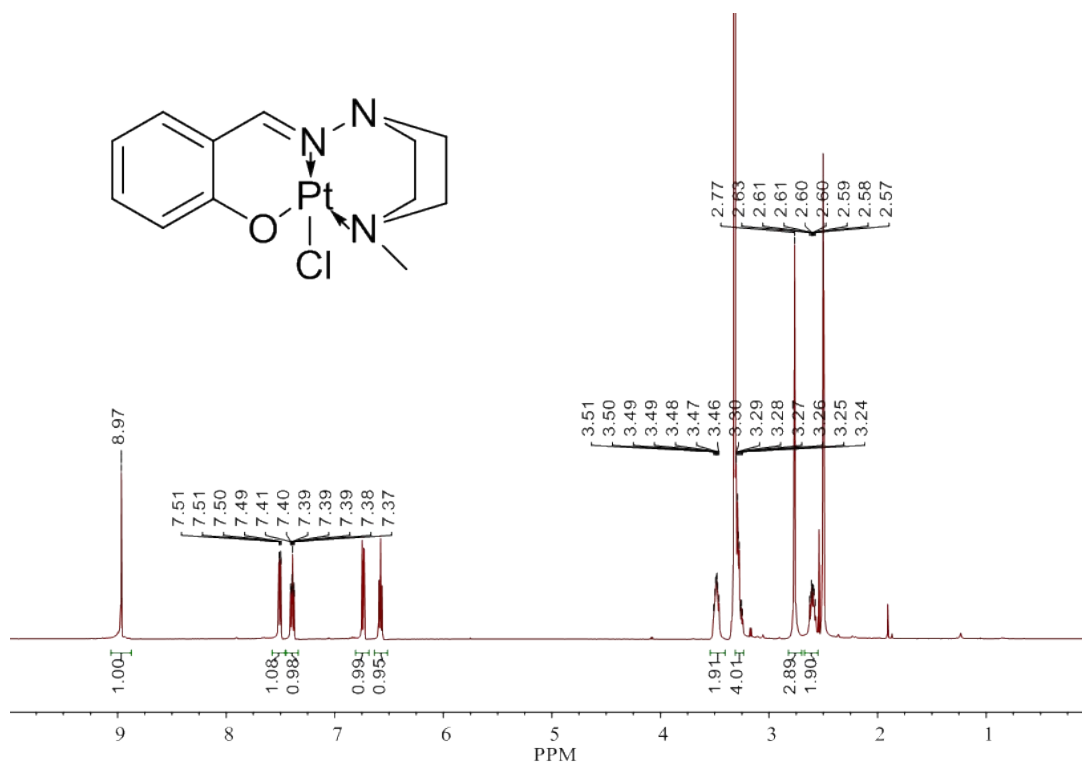


Fig. S17 ^1H NMR of C1 in DMSO- d_6 at 25°C

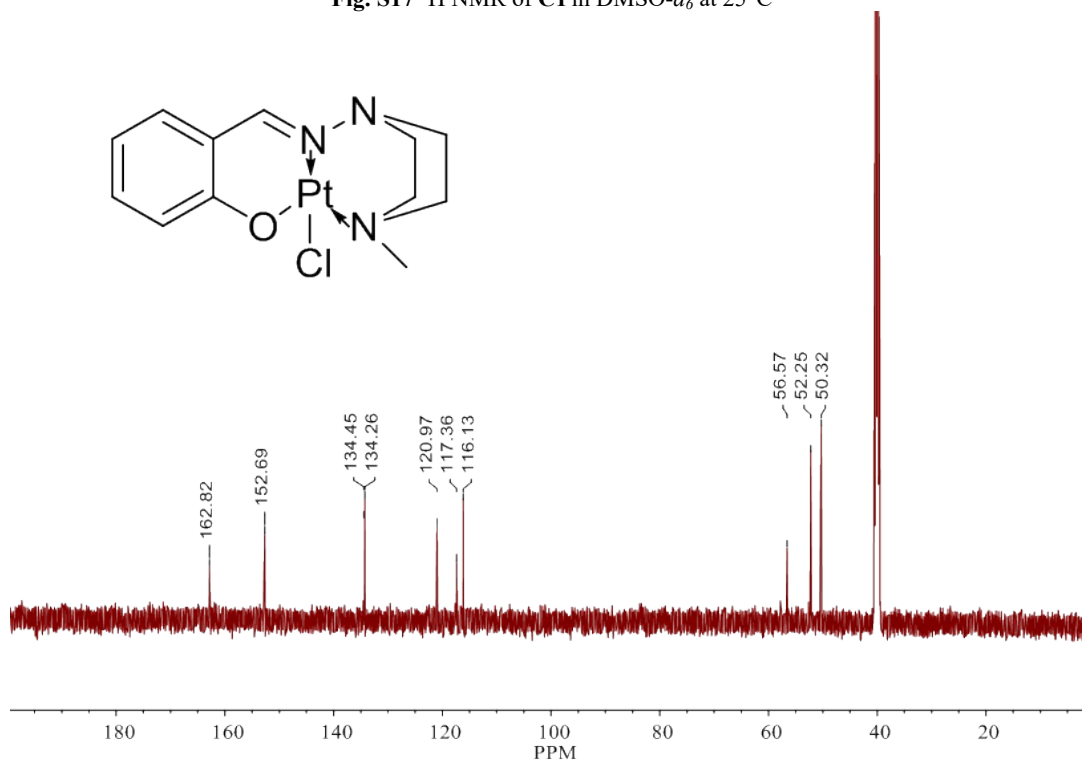


Fig. S18 ^{13}C NMR of C1 in DMSO- d_6 at 25°C

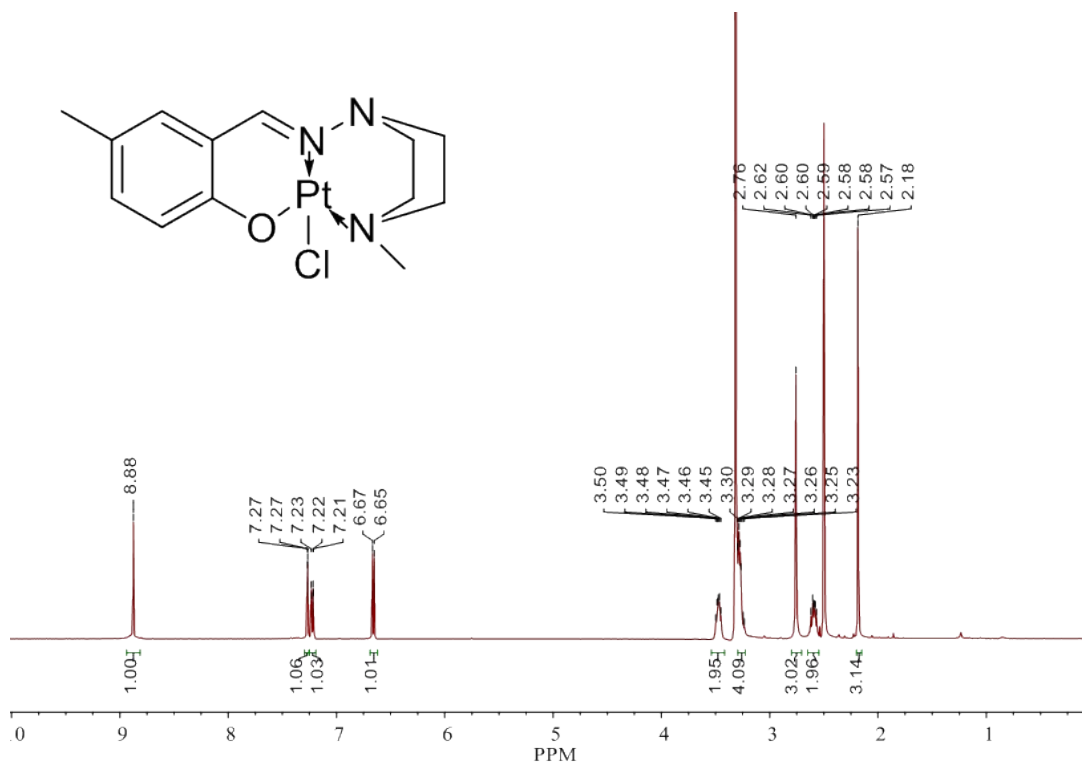


Fig. S19 ¹H NMR of C2 in DMSO-*d*₆ at 25°C

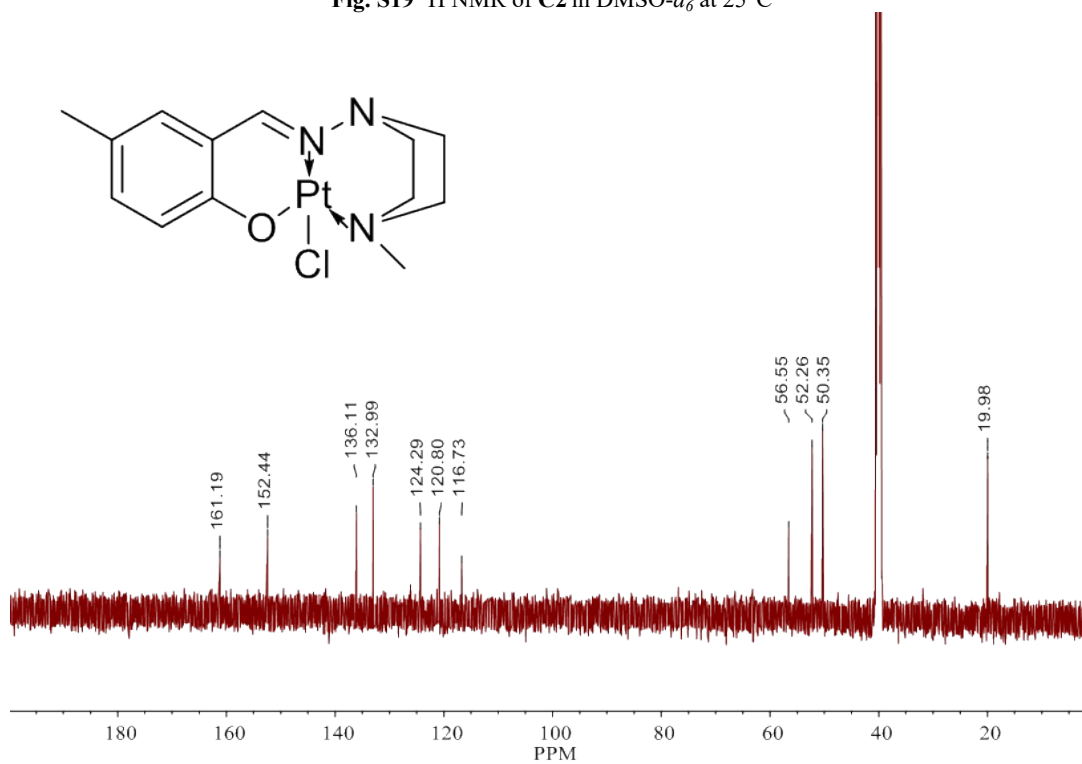


Fig. S20 ¹³C NMR of C2 in DMSO-*d*₆ at 25°C

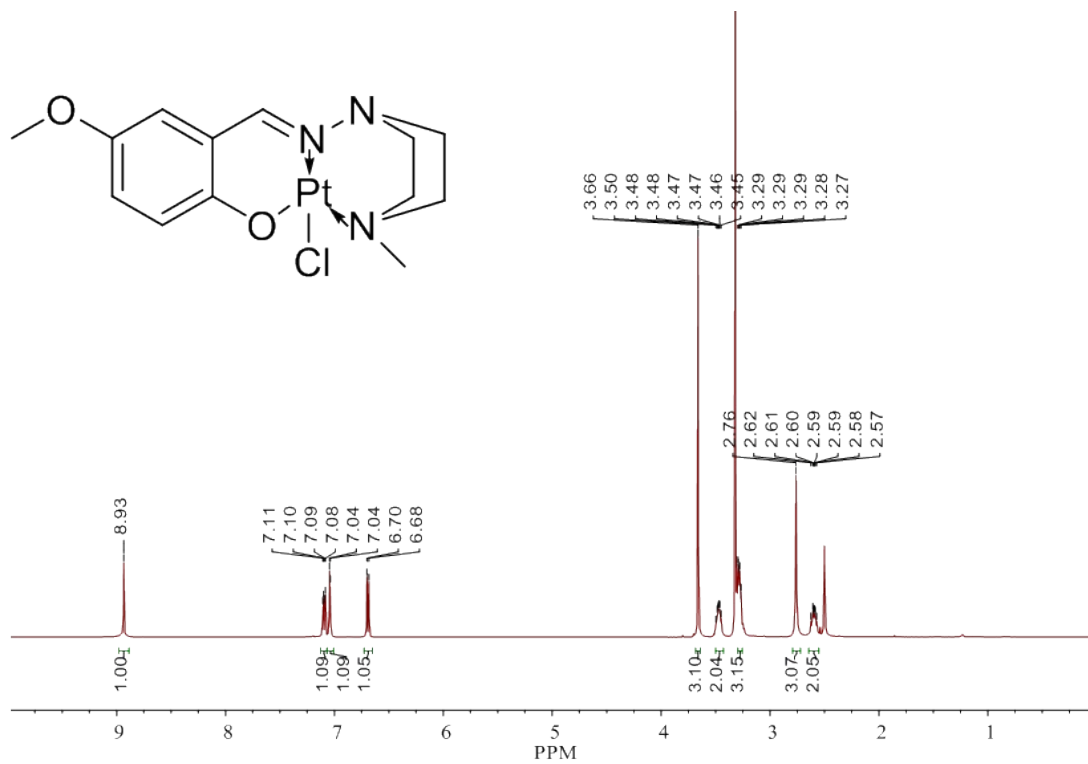


Fig. S21 ¹H NMR of C3 in DMSO-*d*₆ at 25°C

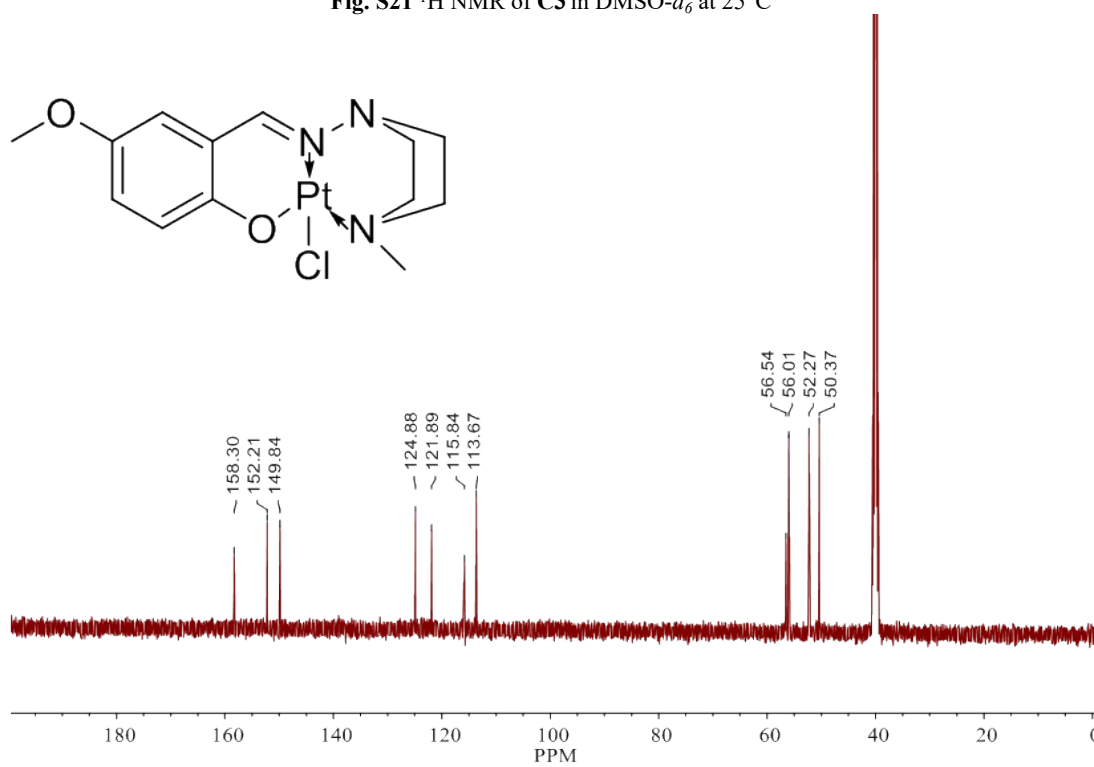


Fig. S22 ^{13}C NMR of C3 in $\text{DMSO-}d_6$ at 25°C

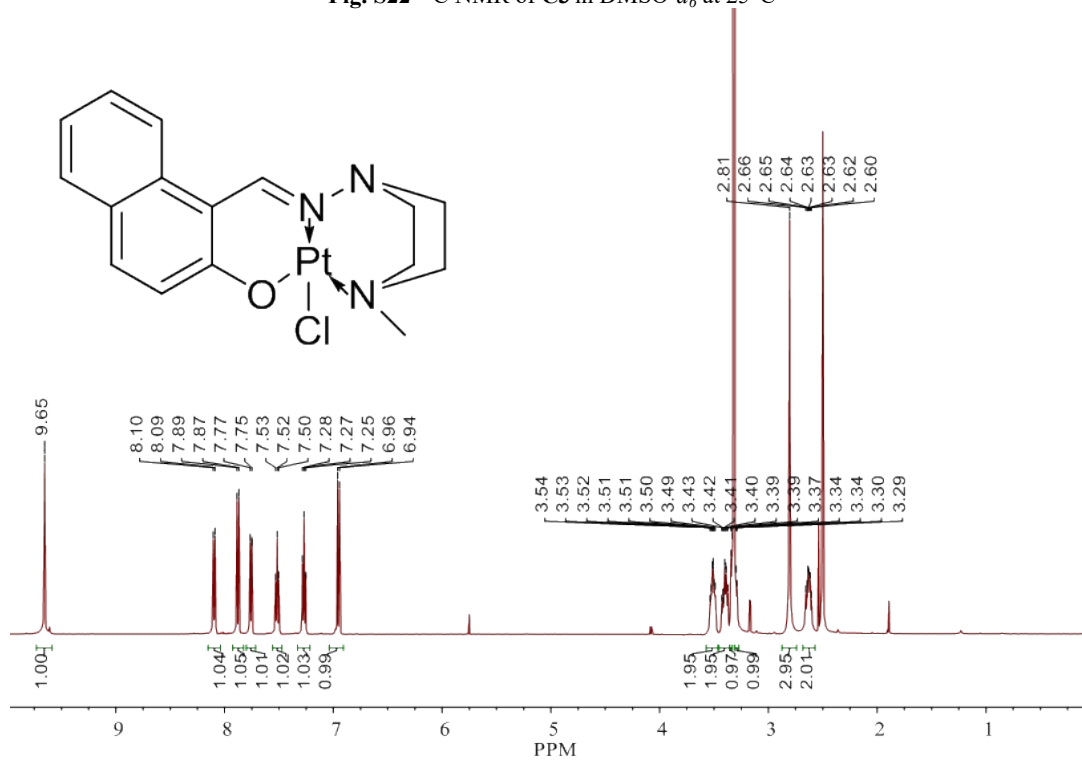


Fig. S23 ^1H NMR of C4 in $\text{DMSO-}d_6$ at 25°C

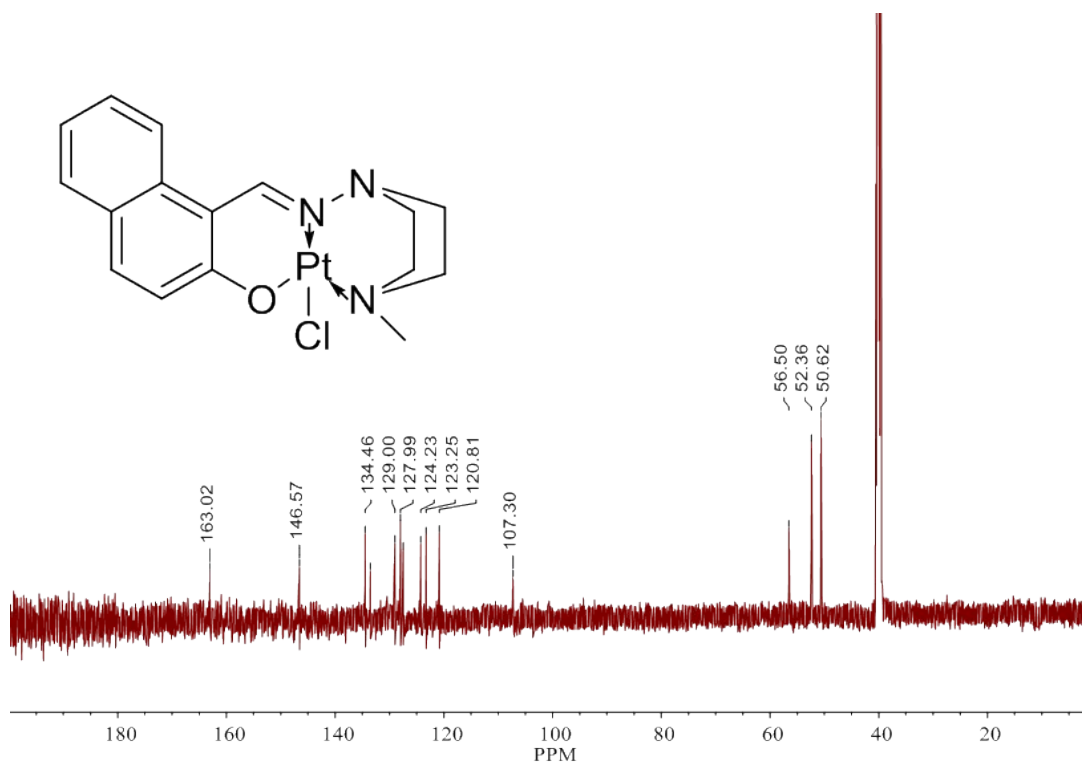


Fig. S24 ^{13}C NMR of C4 in $\text{DMSO-}d_6$ at 25°C

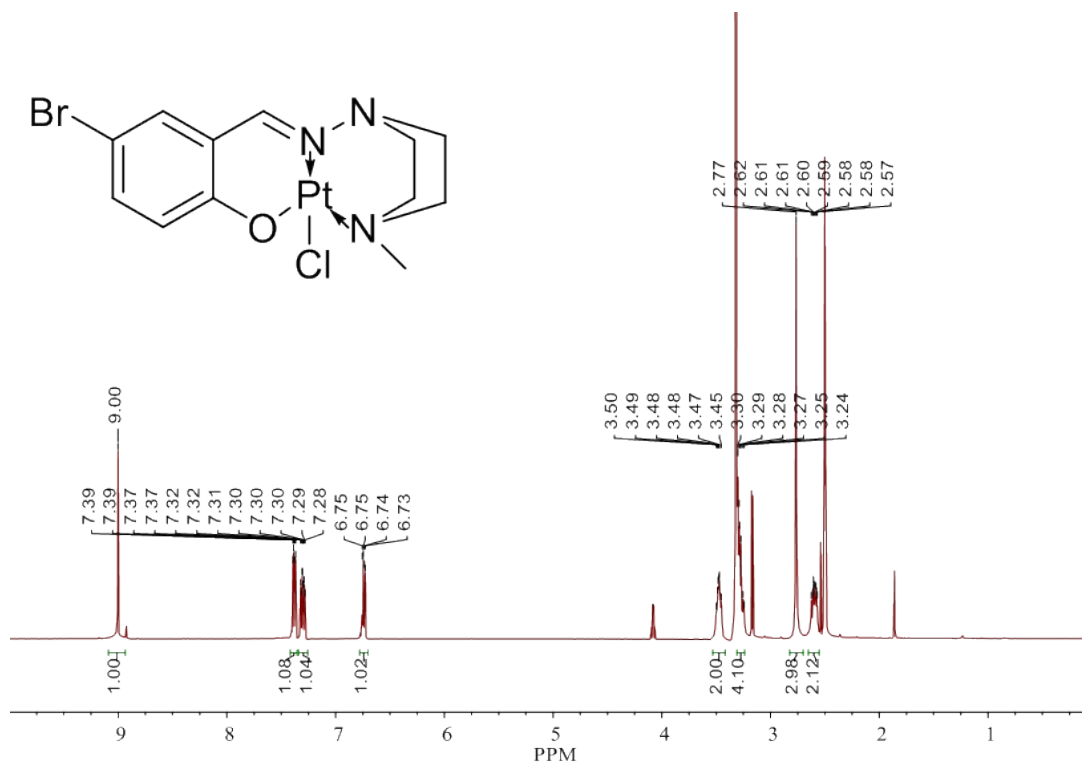


Fig. S25 ¹H NMR of C5 in DMSO-*d*₆ at 25°C

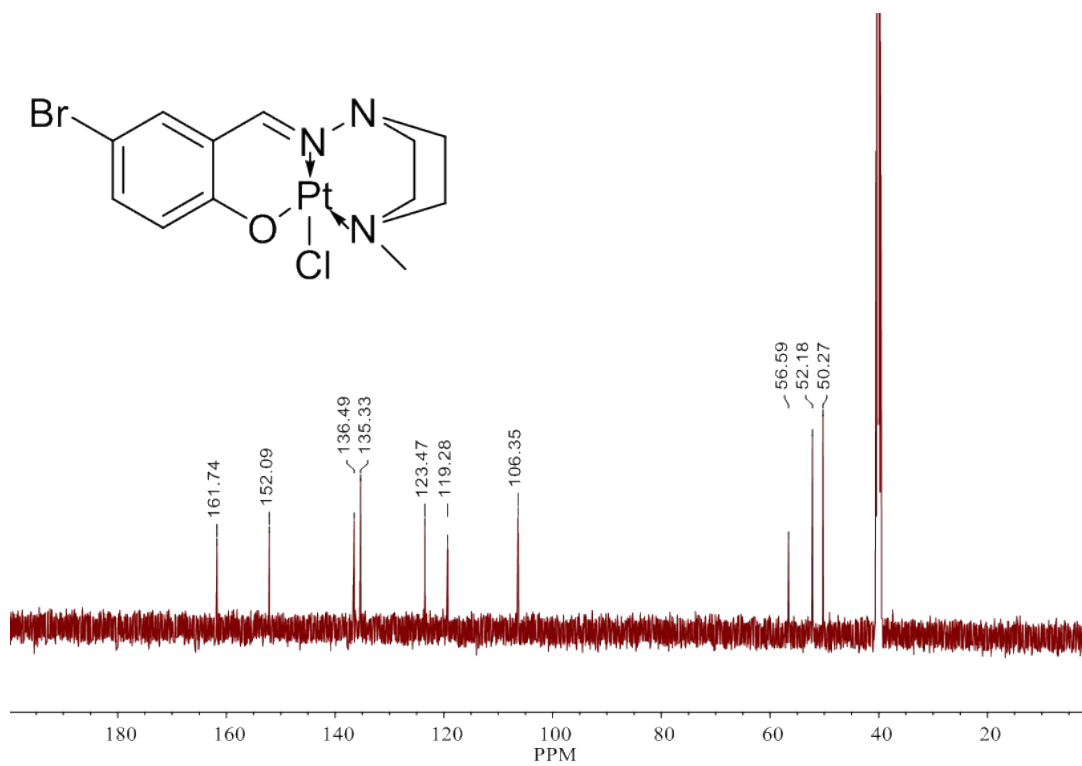


Fig. S26 ¹³C NMR of C5 in DMSO-*d*₆ at 25°C

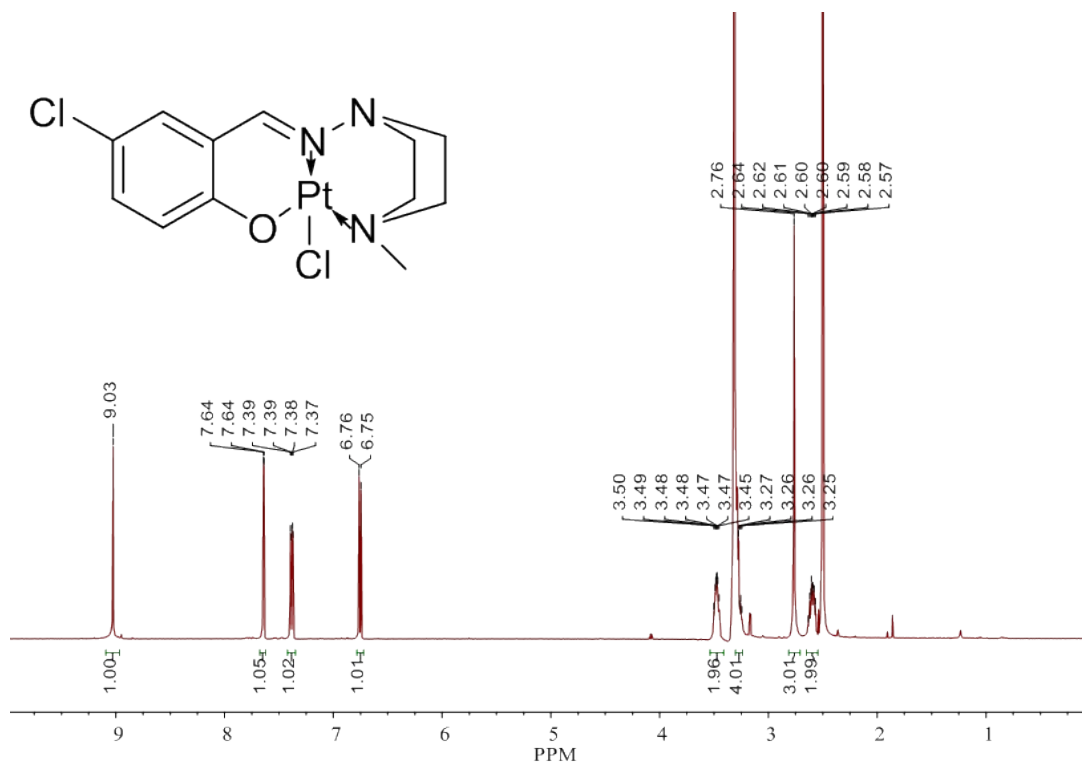


Fig. S27 ^1H NMR of C6 in DMSO- d_6 at 25°C

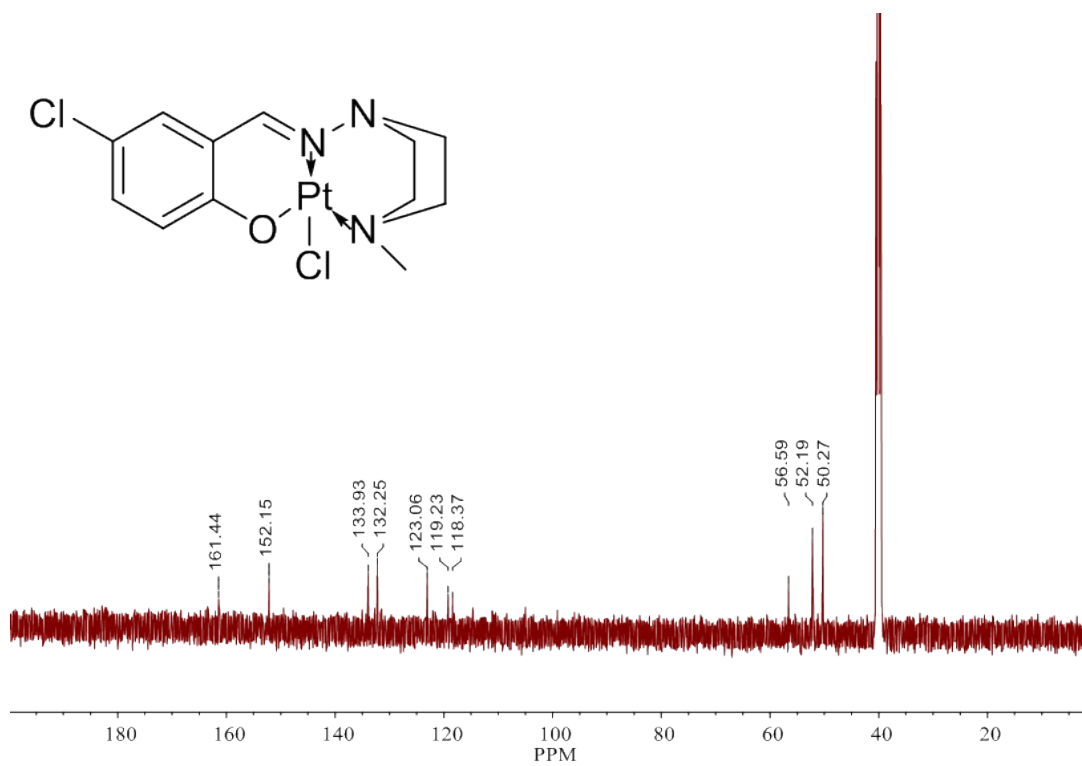


Fig. S28 ^{13}C NMR of C6 in DMSO- d_6 at 25°C

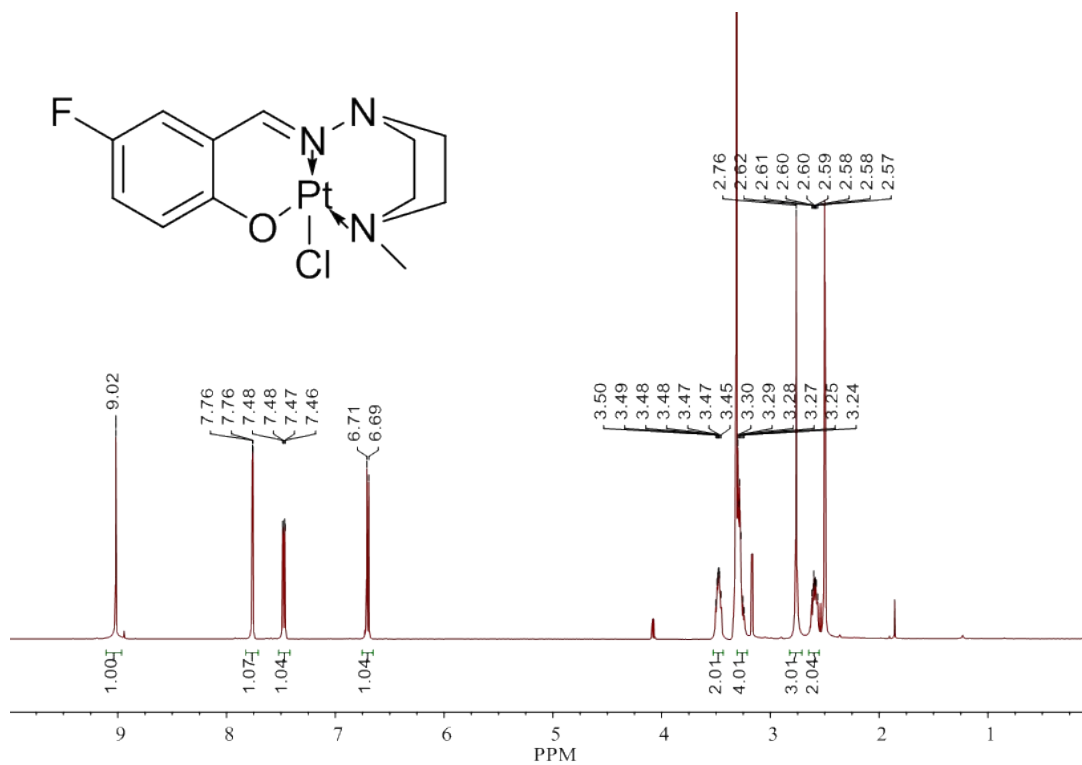


Fig. S29 ¹H NMR of C7 in DMSO-*d*₆ at 25°C

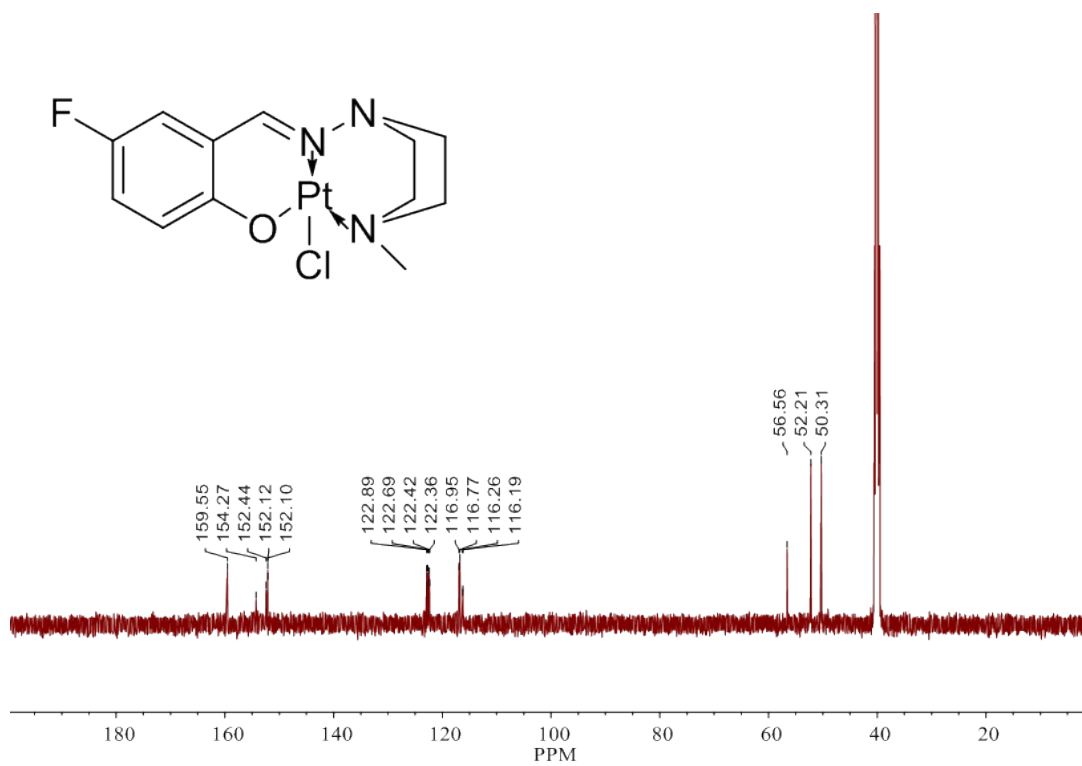


Fig. S30 ¹³C NMR of C7 in DMSO-*d*₆ at 25°C

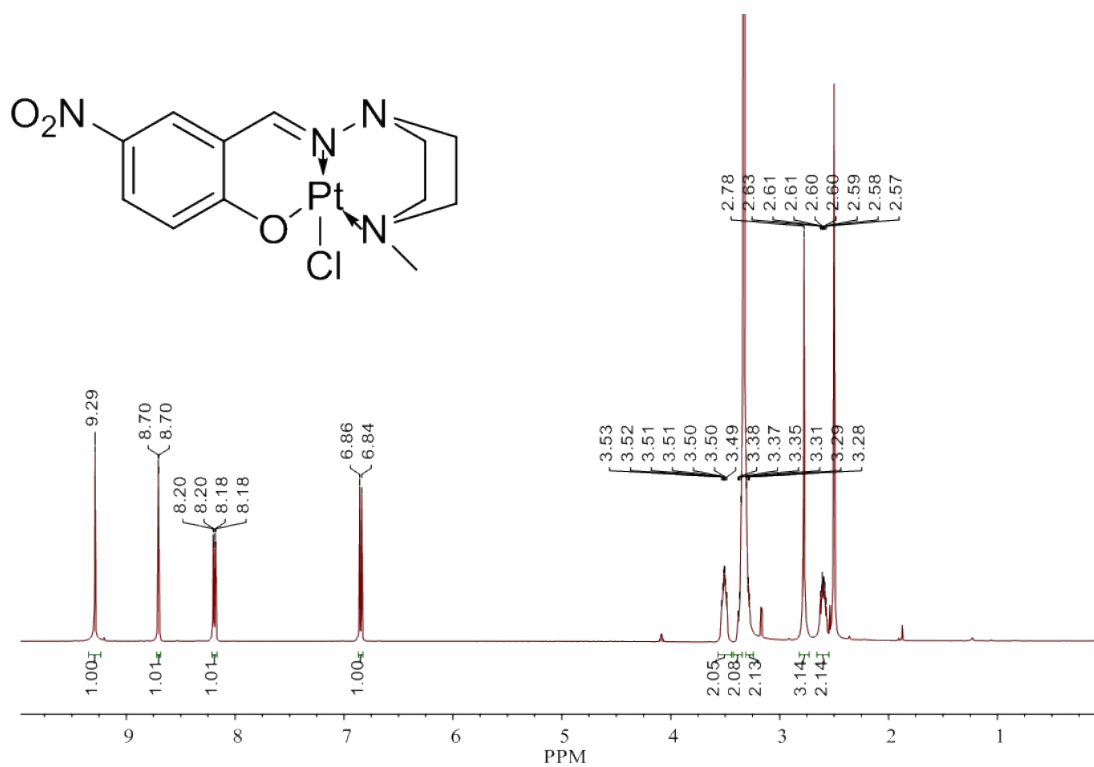


Fig. S31 ¹H NMR of C8 in DMSO-*d*₆ at 25°C

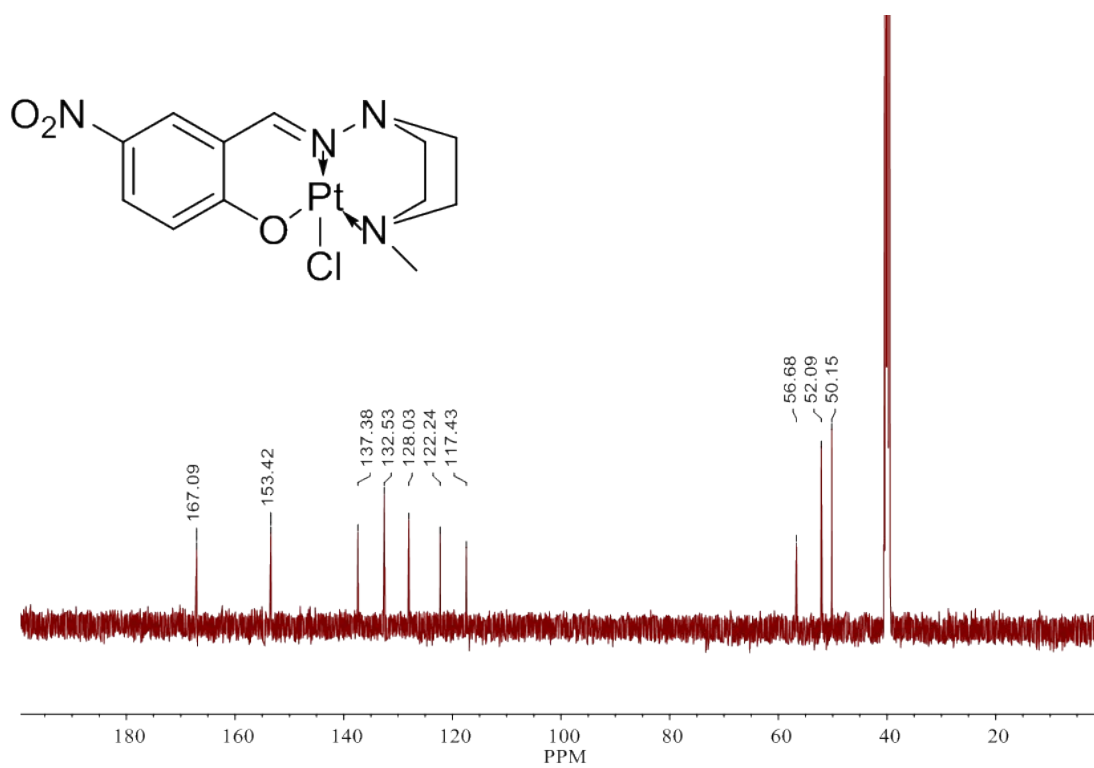


Fig. S32 ¹³C NMR of C8 in DMSO-*d*₆ at 25°C

Mass spectra of all ligands (L1-L8)

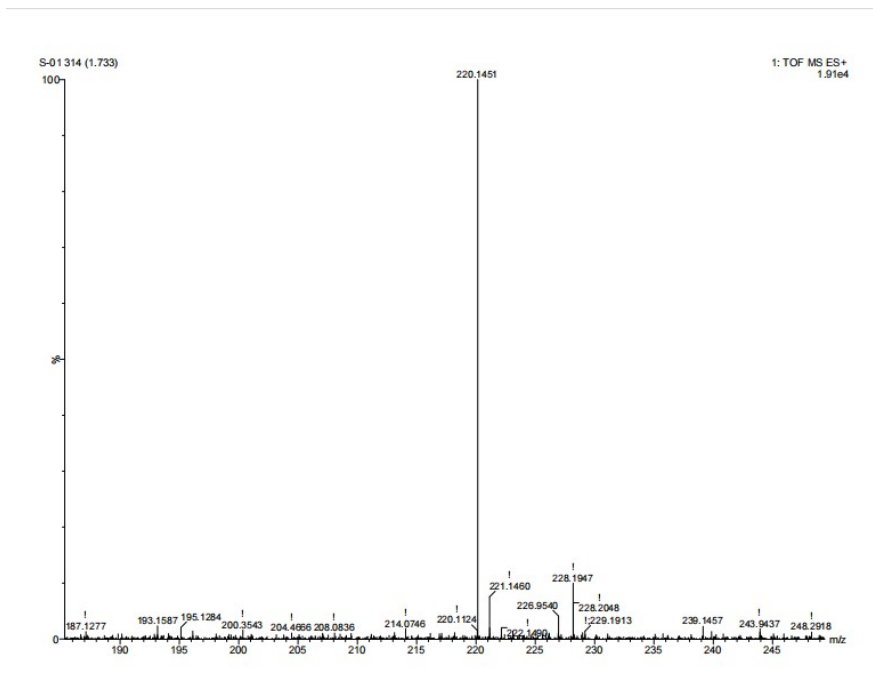


Fig. S33 Mass Spectrum of L1

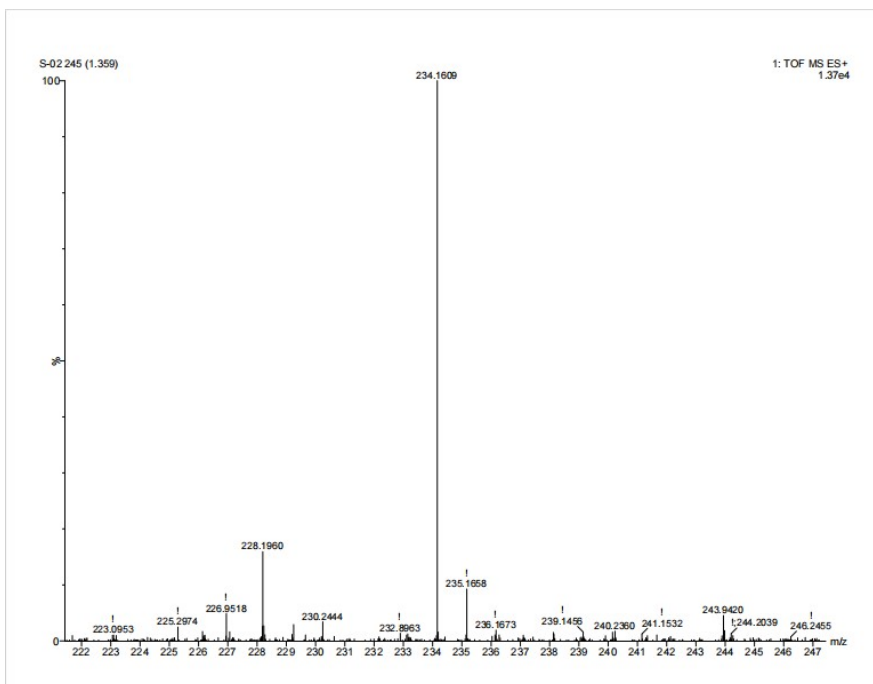


Fig. S34 Mass Spectrum of L2

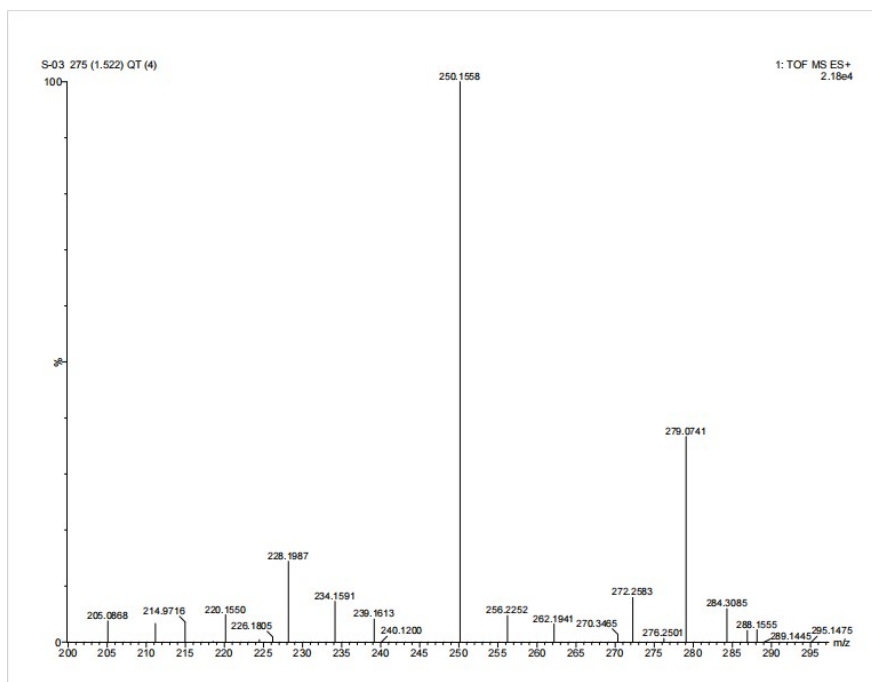


Fig. S35 Mass Spectrum of L3

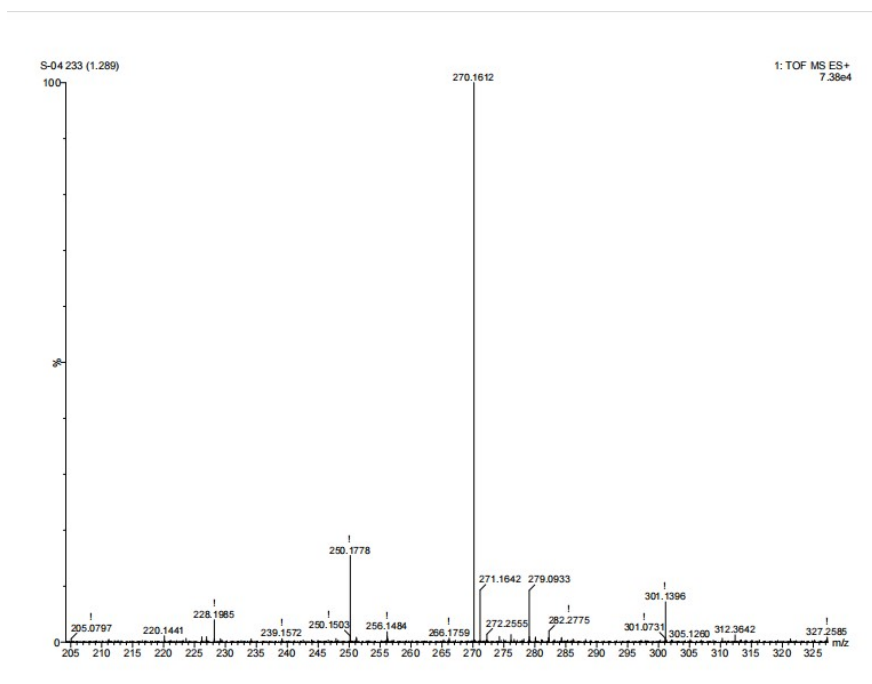


Fig. S36 Mass Spectrum of L4

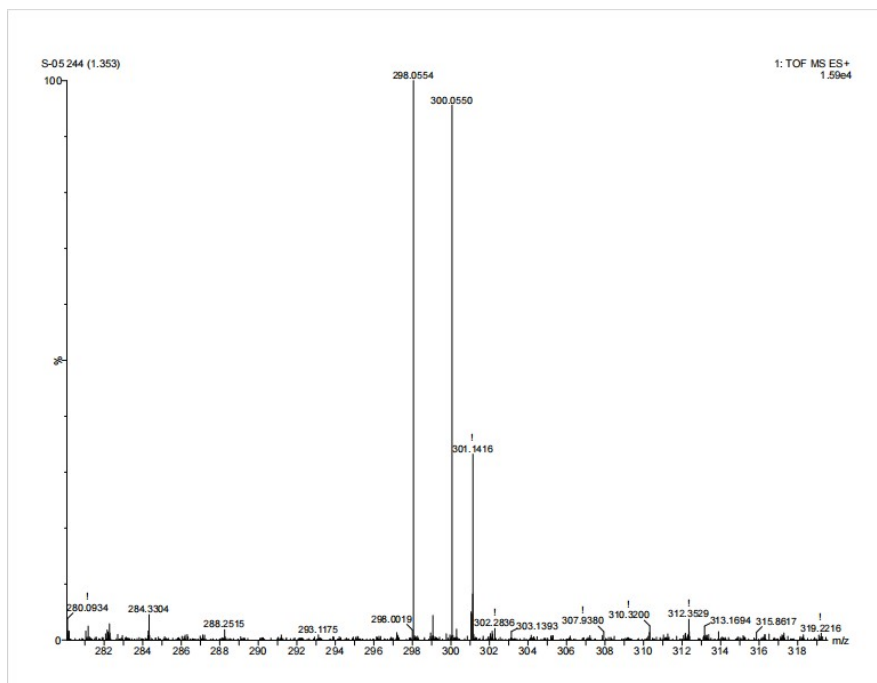


Fig. S37 Mass Spectrum of L5

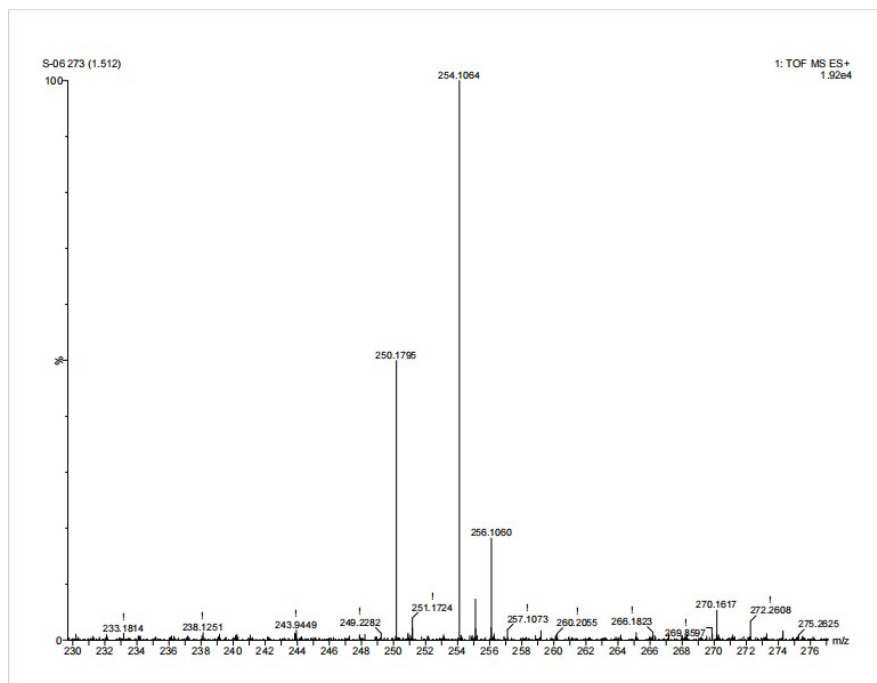


Fig. S38 Mass Spectrum of L6

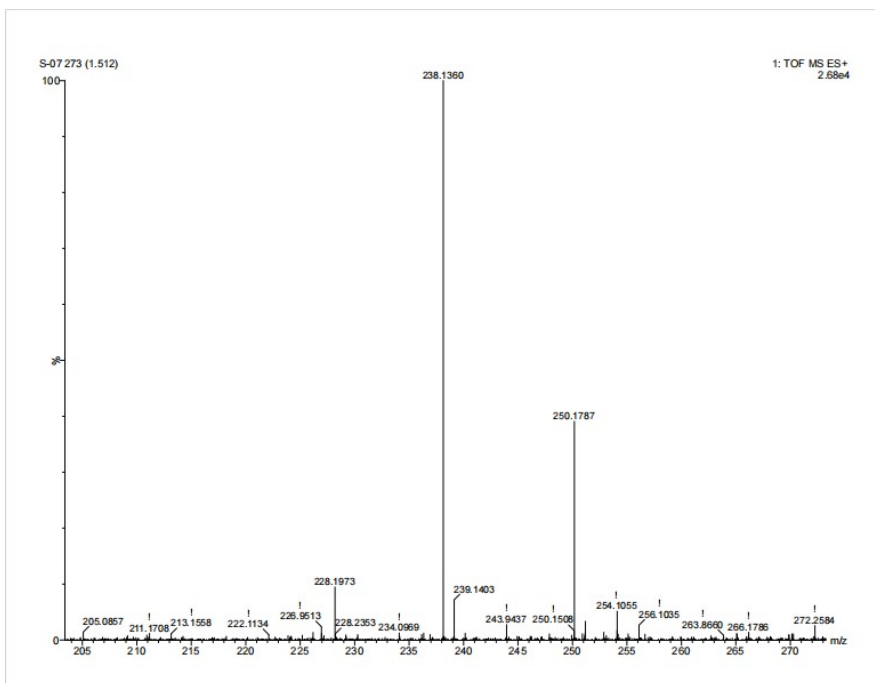


Fig. S39 Mass Spectrum of L7

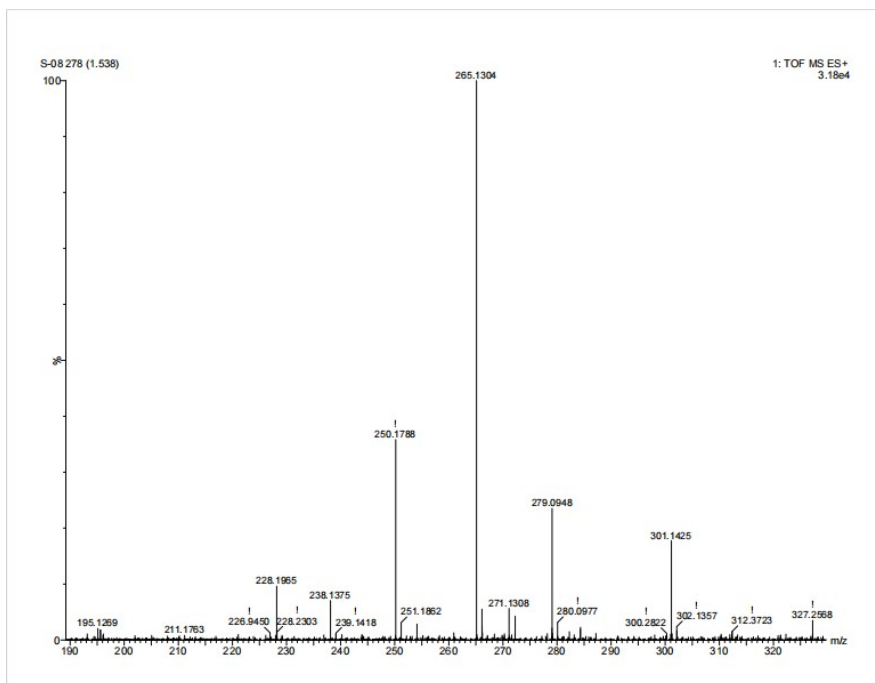


Fig. S40 Mass Spectrum of L8

Mass spectra of all platinum complexes (C1-C8)

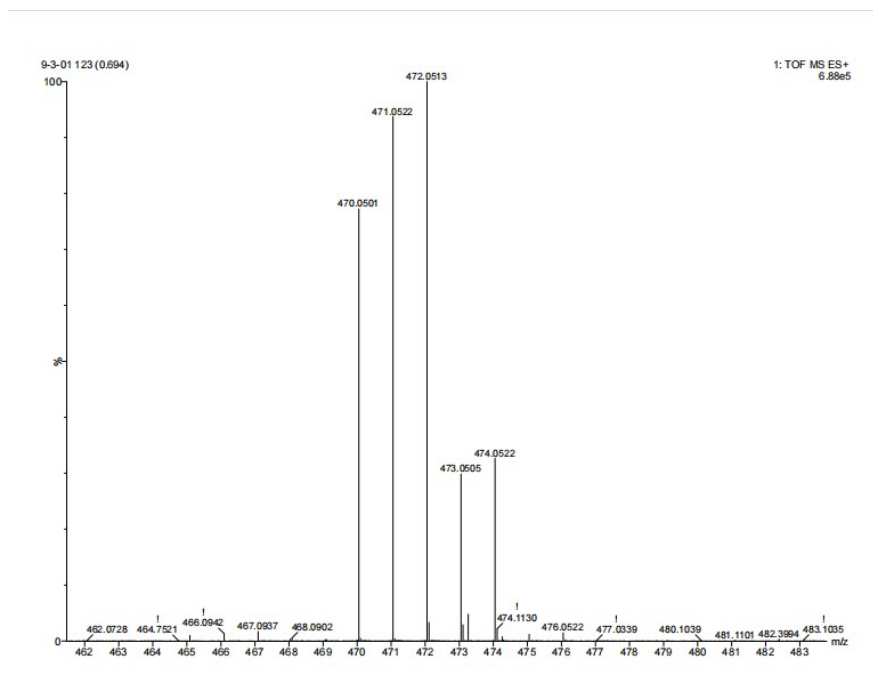


Fig. S41 Mass Spectrum of C1

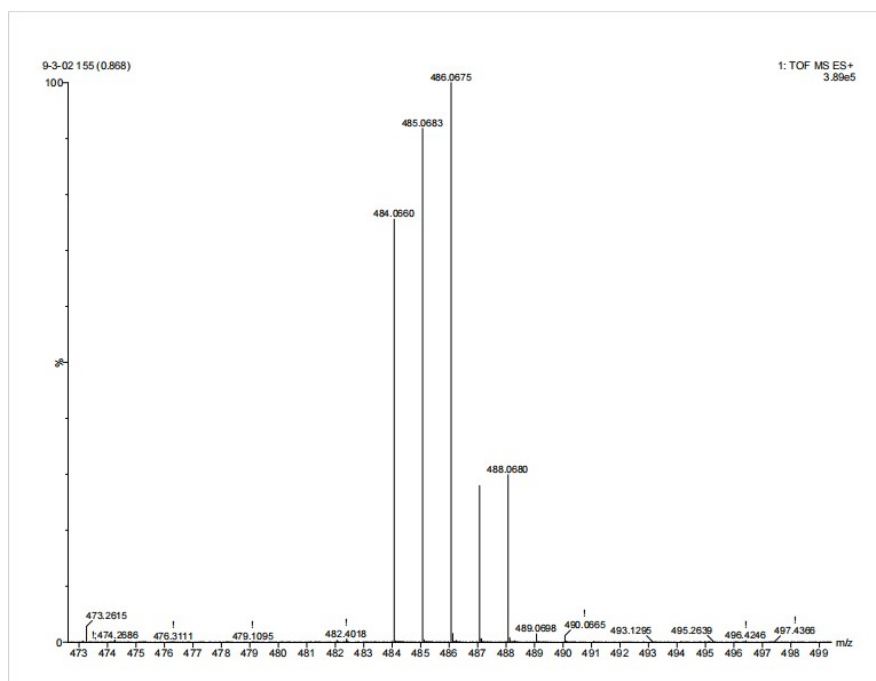


Fig. S42 Mass Spectrum of C2

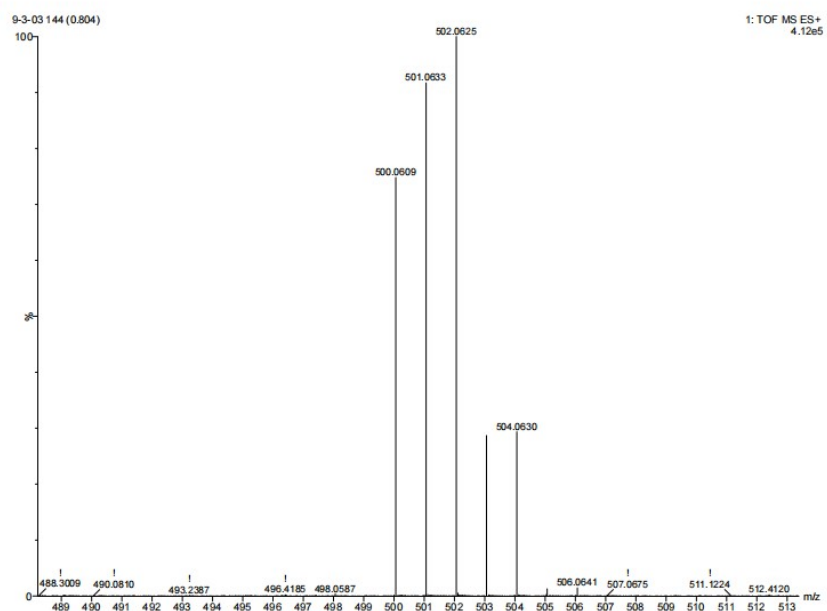


Fig. S43 Mass Spectrum of C3

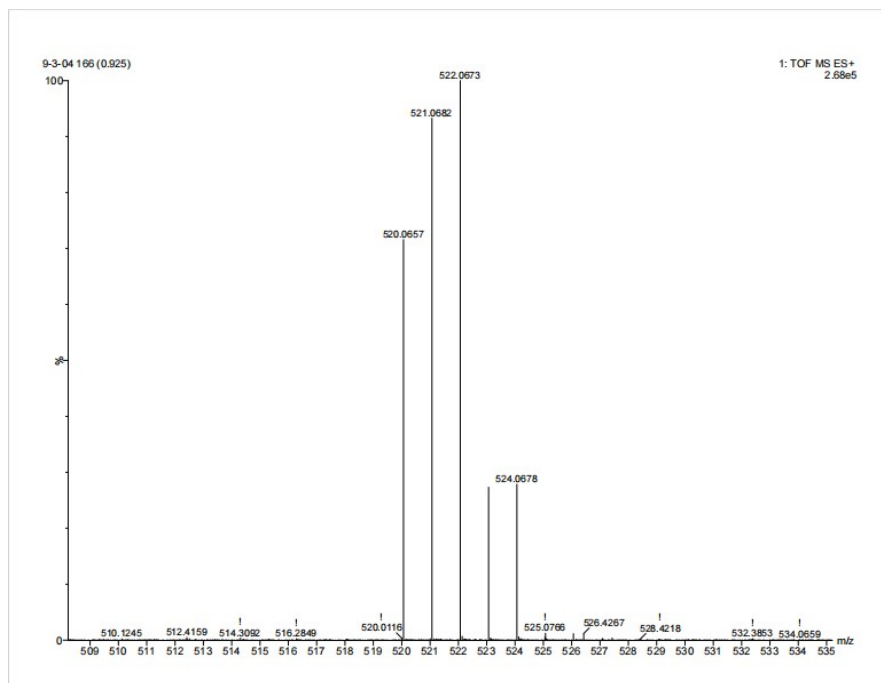


Fig. S44 Mass Spectrum of C4

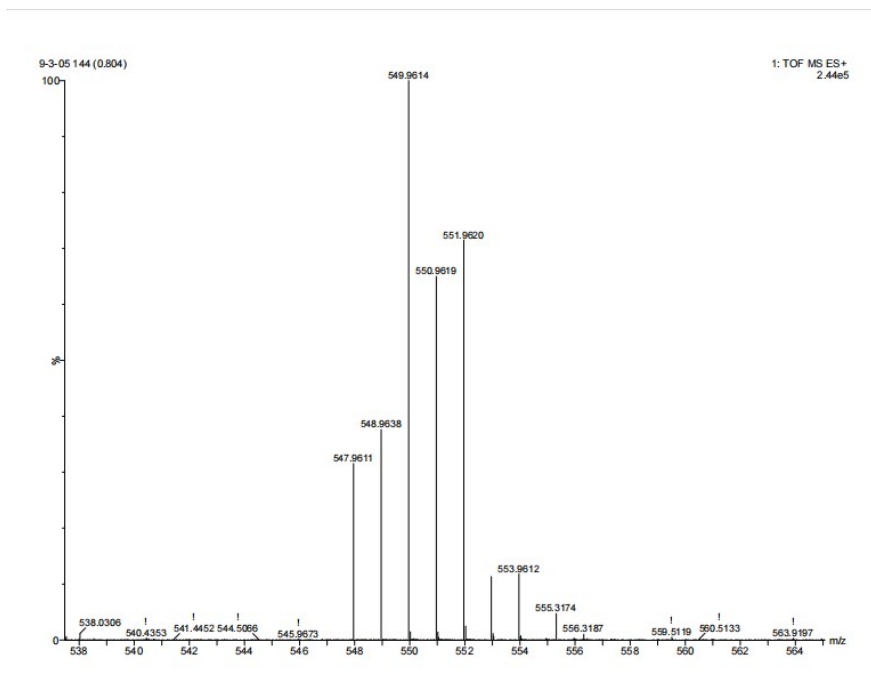


Fig. S45 Mass Spectrum of C5

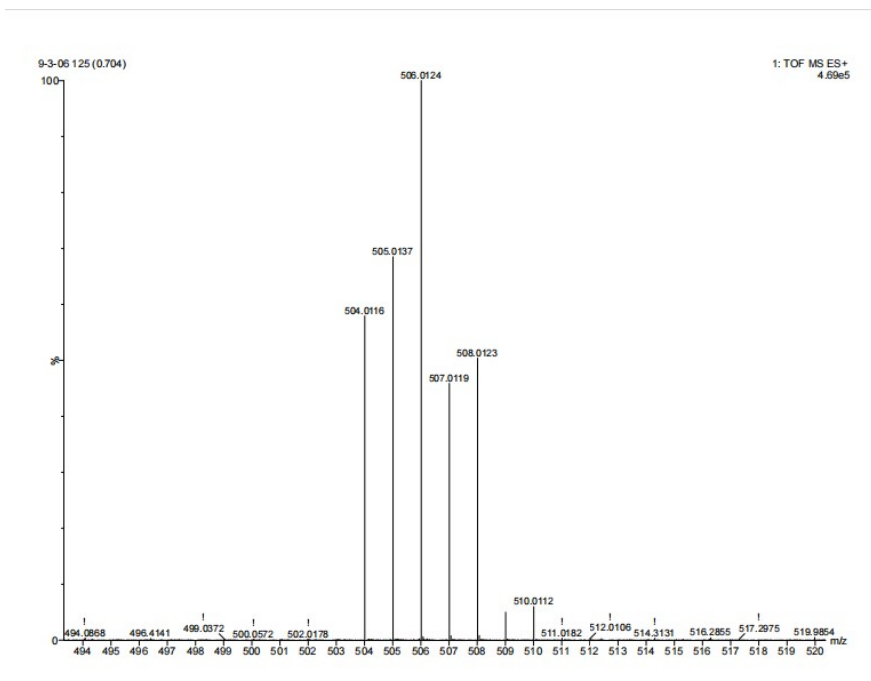


Fig. S46 Mass Spectrum of C6

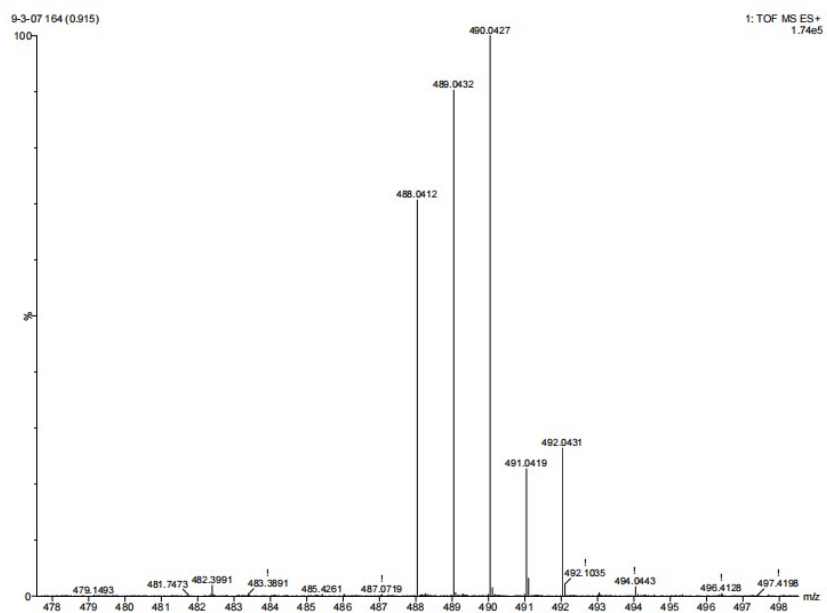


Fig. S47 Mass Spectrum of C7

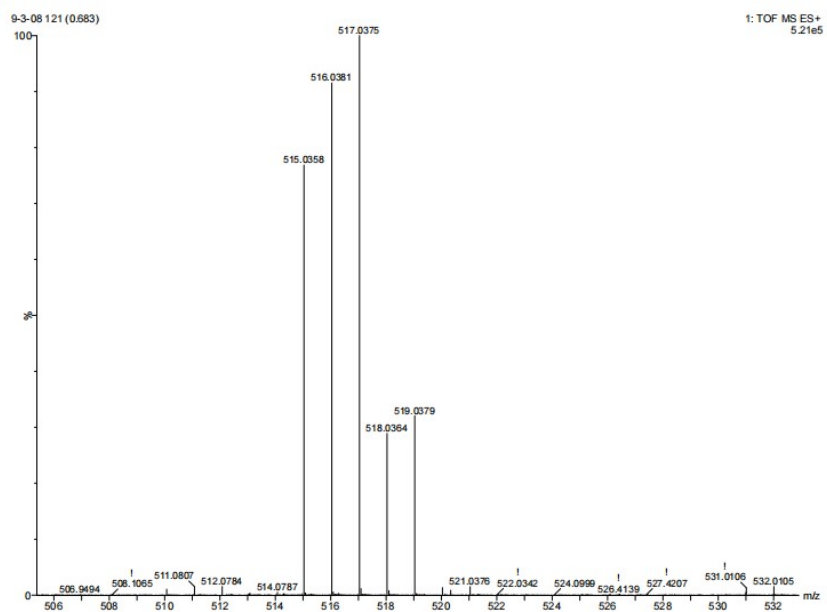


Fig. S48 Mass Spectrum of C8

FT-IR Spectra of L1-L8 and L1-L8 and C1-C8

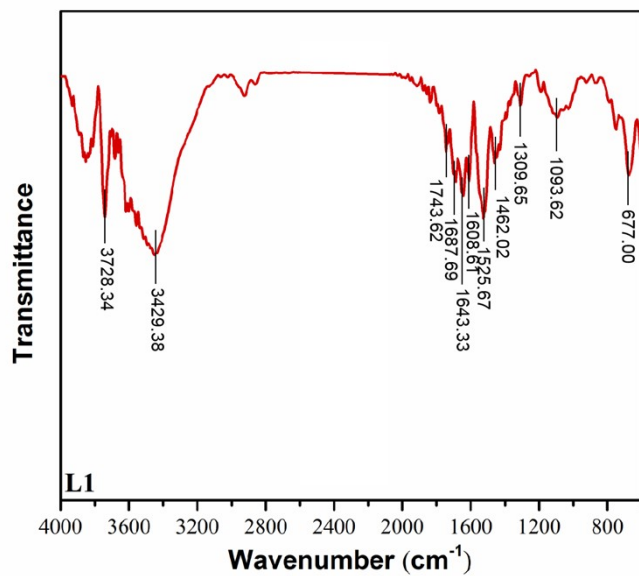


Fig. S49 FT-IR Spectrum of L1

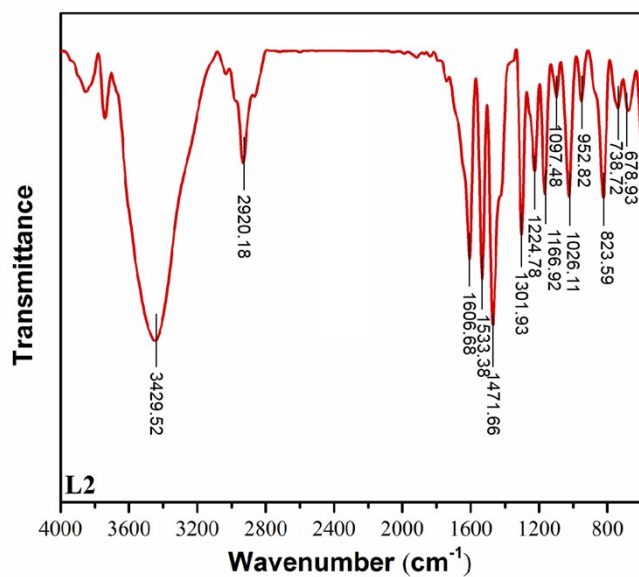


Fig. S50 FT-IR Spectrum of L2

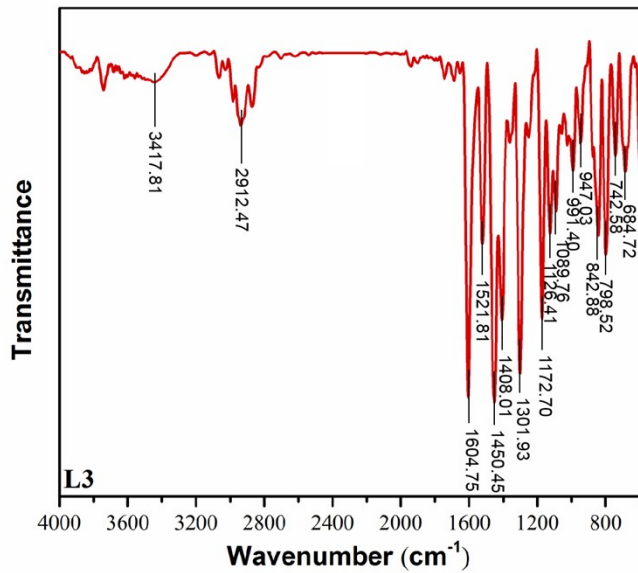


Fig. S51 FT-IR Spectrum of L3

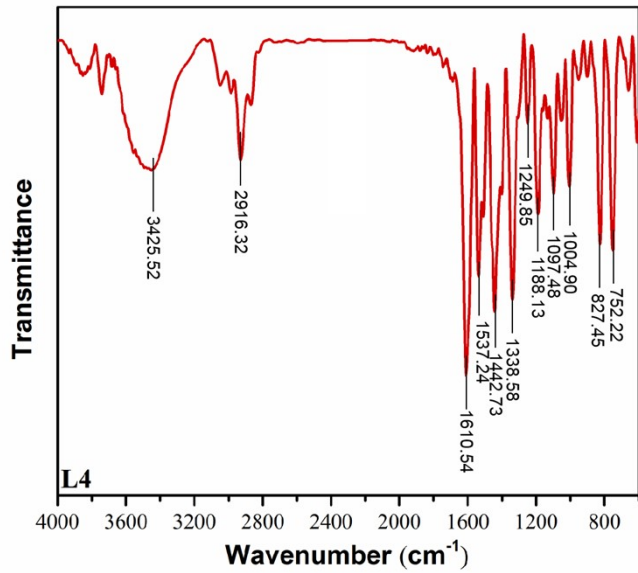


Fig. S52 FT-IR Spectrum of L4

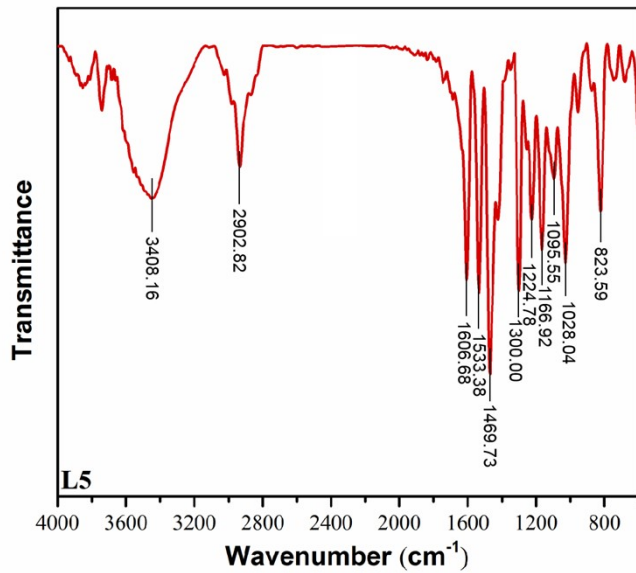


Fig. S53 FT-IR Spectrum of L5

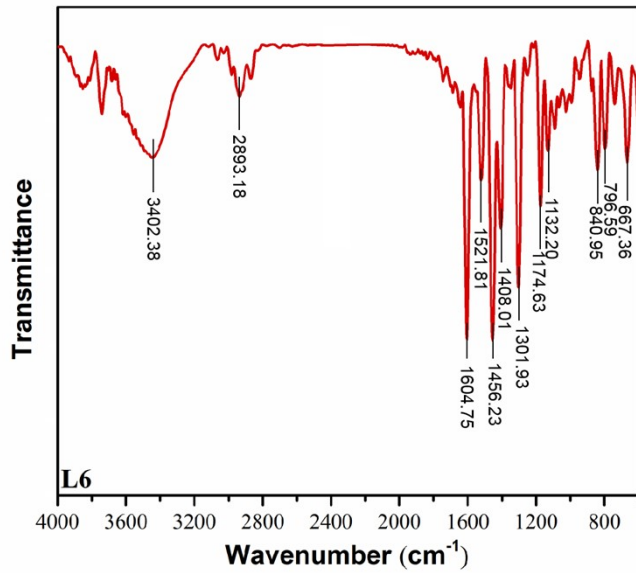


Fig. S54 FT-IR Spectrum of L6

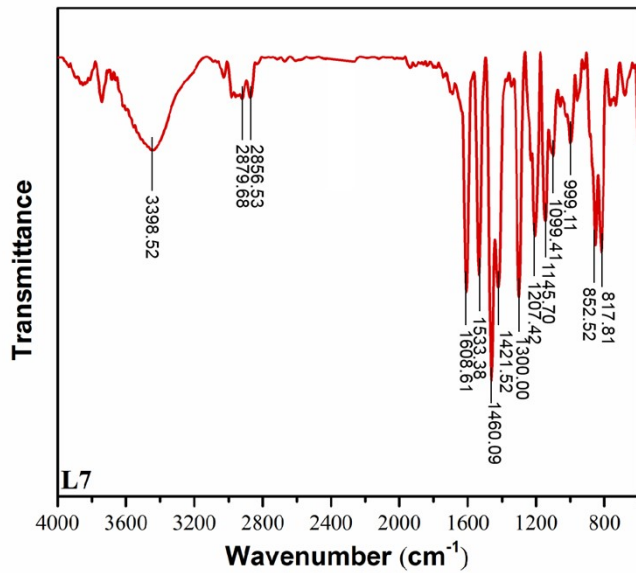


Fig. S55 FT-IR Spectrum of L7

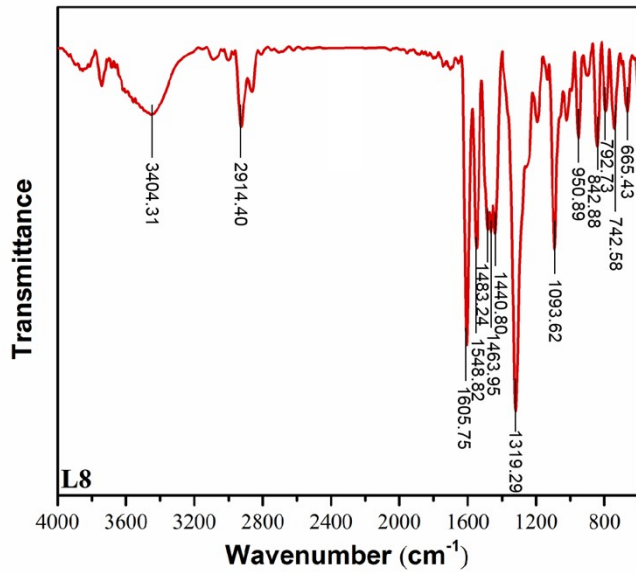


Fig. S56 FT-IR Spectrum of L8

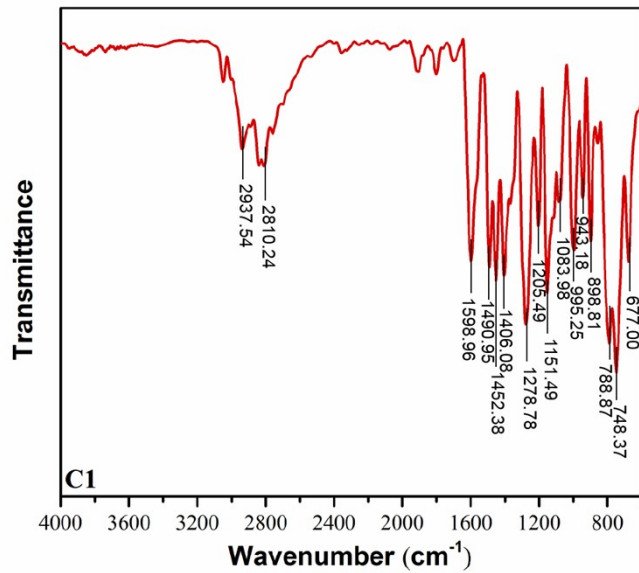


Fig. S57 FT-IR Spectrum of C1

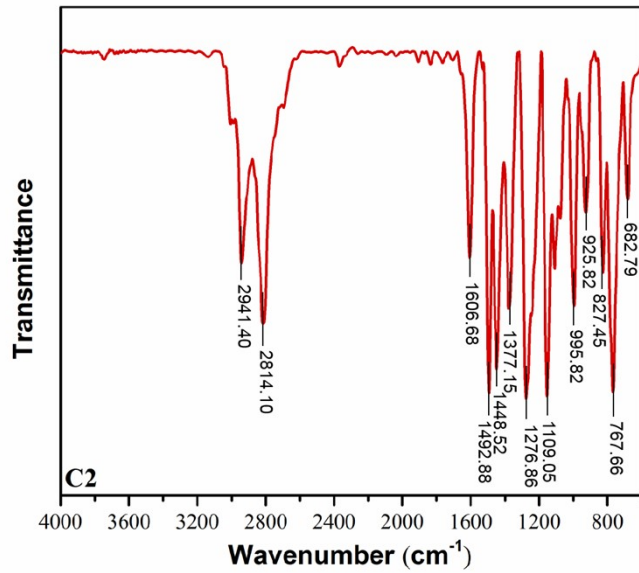


Fig. S58 FT-IR Spectrum of C2

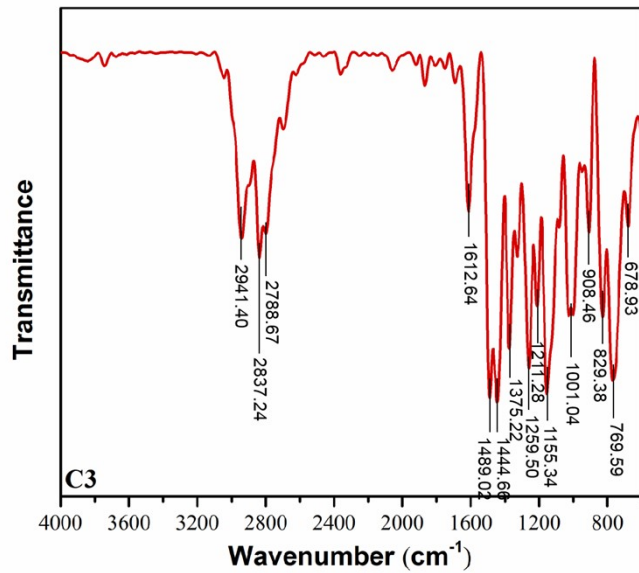


Fig. S59 FT-IR Spectrum of C3

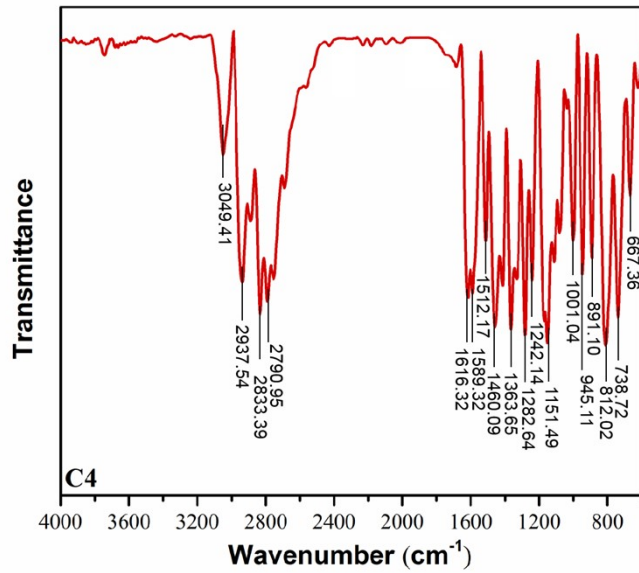


Fig. S60 FT-IR Spectrum of C4

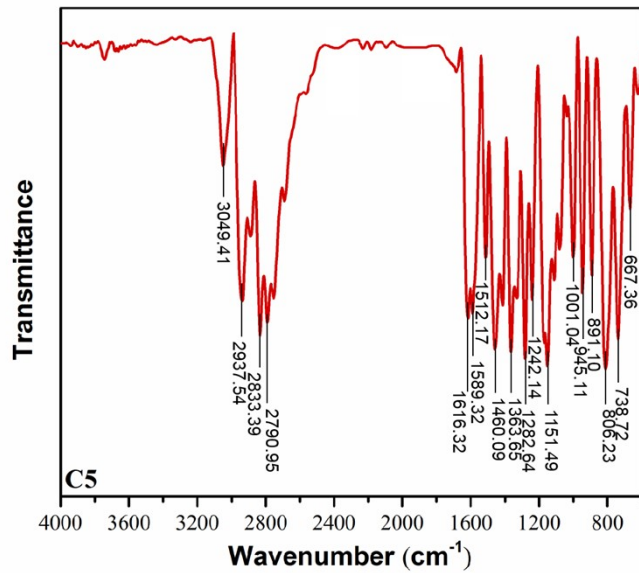


Fig. S61 FT-IR Spectrum of C5

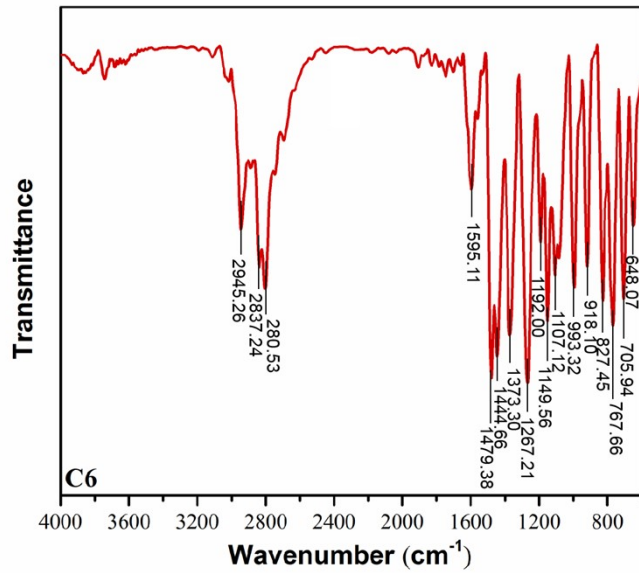


Fig. S62 FT-IR Spectrum of C6

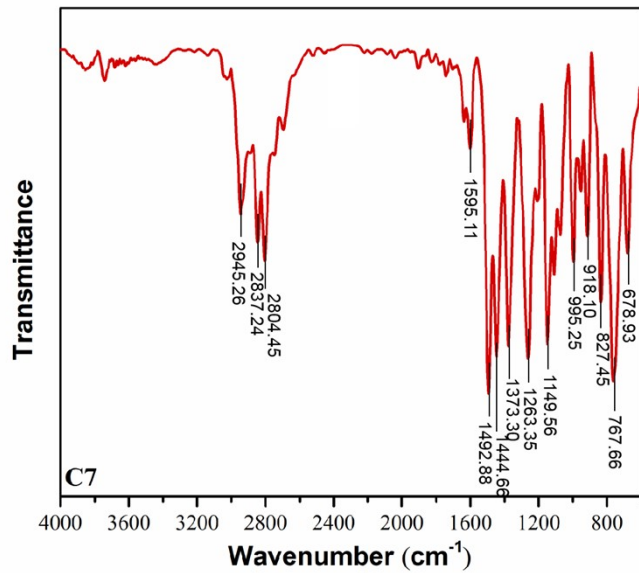


Fig. S63 FT-IR Spectrum of C7

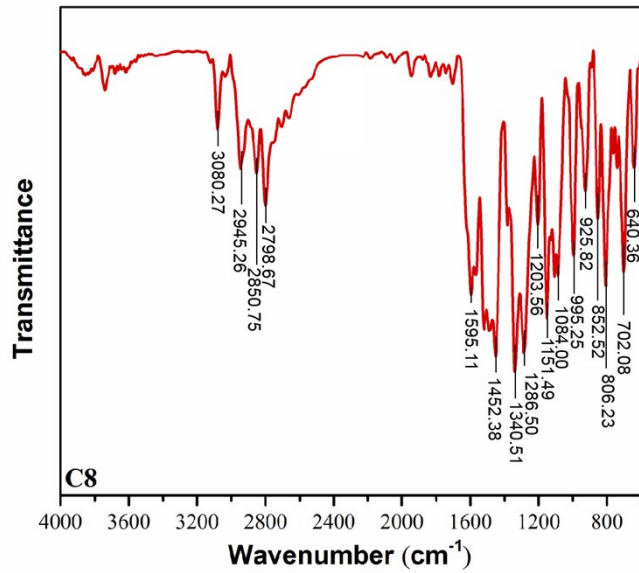


Fig. S64 FT-IR Spectrum of C8

Stability analysis of C3, C4, C5 and C6

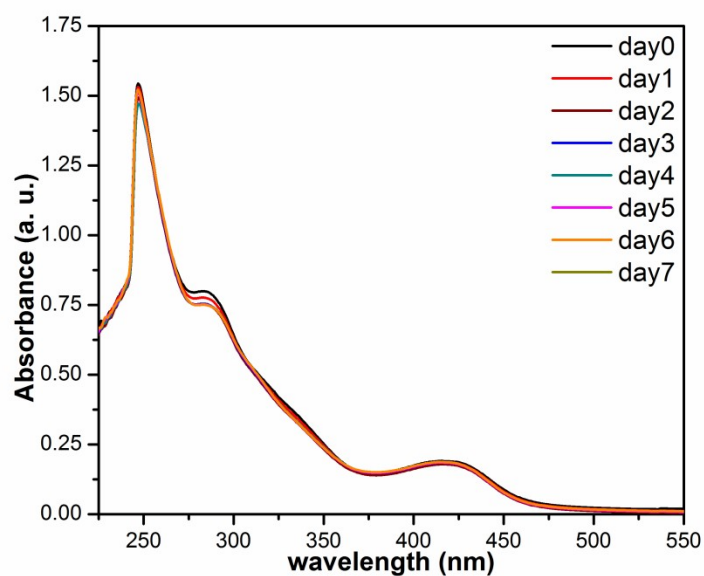


Fig. S65 UV-vis spectra of the stability analyses of C3 in DMSO:H₂O=1:1, over the mentioned time points

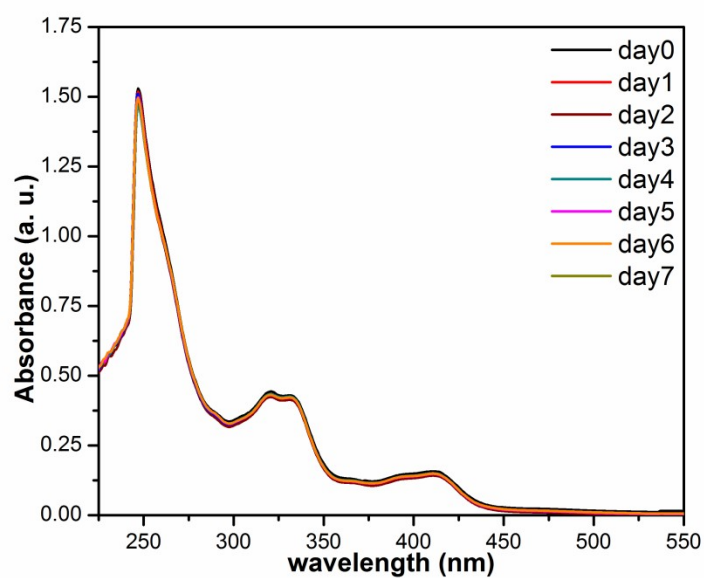


Fig. S66 UV-vis spectra of the stability analyses of C4 in DMSO:H₂O=1:1, over the mentioned time points

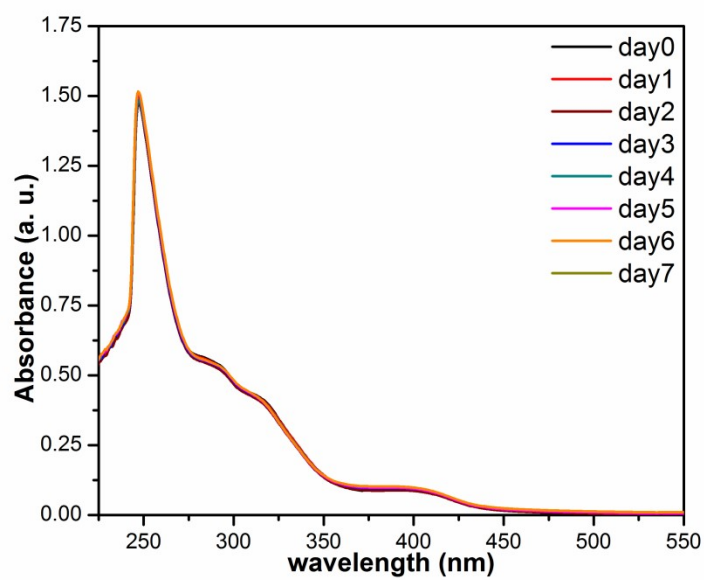


Fig. S67 UV-vis spectra of the stability analyses of C5 in DMSO:H₂O=1:1, over the mentioned time points

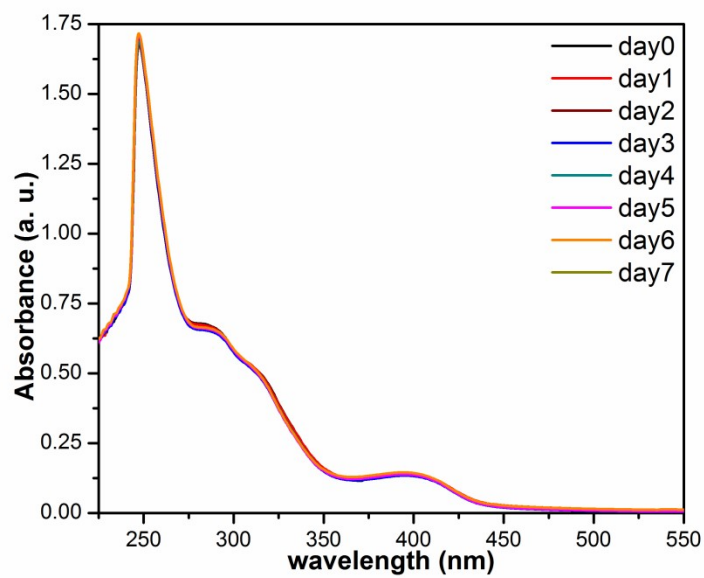


Fig. S68 UV-vis spectra of the stability analyses of C6 in DMSO:H₂O=1:1, over the mentioned time points

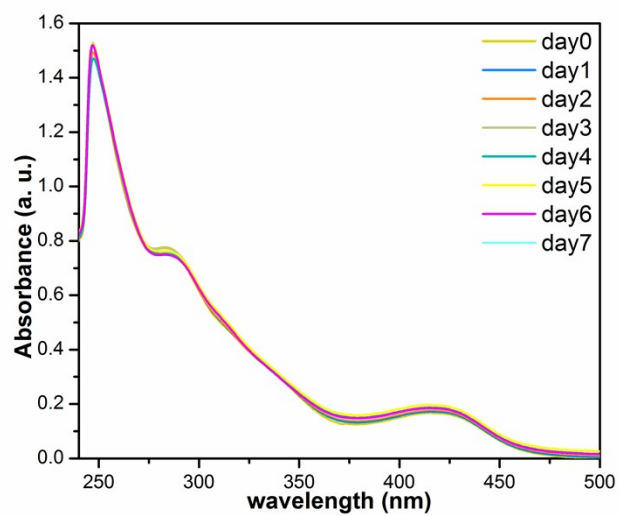


Fig. S69 UV-vis spectra of the stability analyses of C3 in DMSO:PBS=1:1, over the mentioned time points

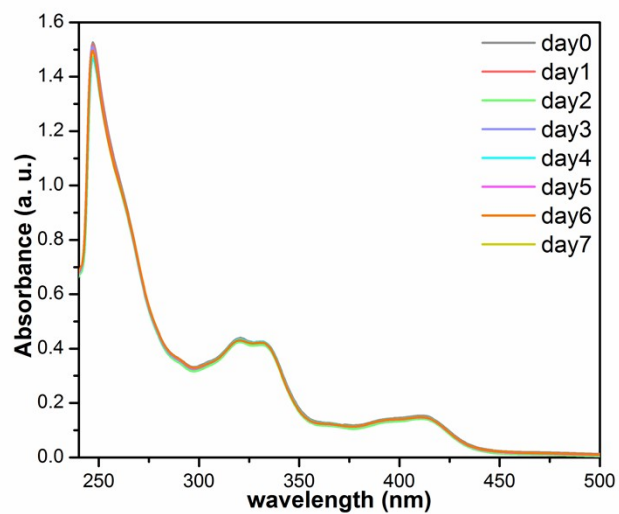


Fig. S70 UV-vis spectra of the stability analyses of C4 in DMSO:PBS=1:1, over the mentioned time points

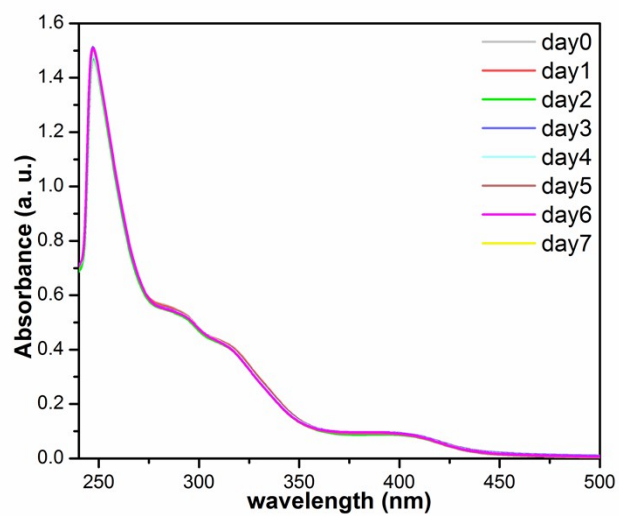


Fig. S71 UV-vis spectra of the stability analyses of C5 in DMSO:PBS=1:1, over the mentioned time points

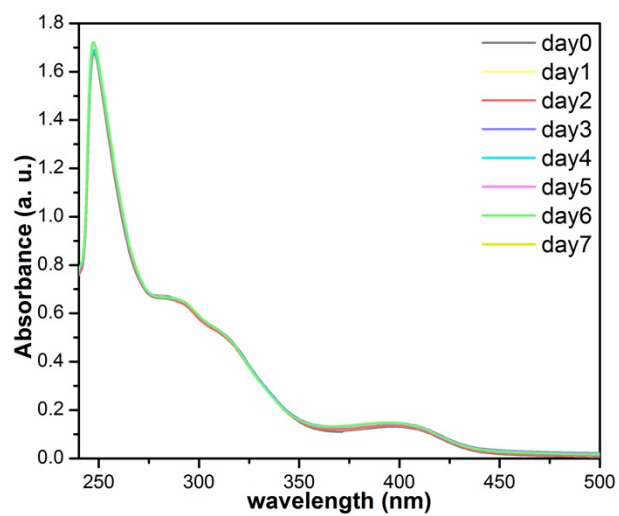


Fig. S72 UV-vis spectra of the stability analyses of C6 in DMSO:PBS=1:1, over the mentioned time points